

# Ring states in topological materials

Raquel Queiroz,<sup>1,2,\*</sup> Roni Ilan,<sup>3</sup> Zhida Song,<sup>4,5</sup> B. Andrei Bernevig,<sup>5,6,7</sup> and Ady Stern<sup>8</sup>

<sup>1</sup>*Department of Physics, Columbia University, New York, NY 10027, USA*

<sup>2</sup>*Center for Computational Quantum Physics, Flatiron Institute, New York, New York 10010, USA*

<sup>3</sup>*Raymond and Beverly Sackler School of Physics and Astronomy, Tel Aviv University, Tel Aviv, Israel*

<sup>4</sup>*International Center for Quantum Materials, School of Physics, Peking University, Beijing, China*

<sup>5</sup>*Department of Physics, Princeton University, Princeton, NJ 08544, USA*

<sup>6</sup>*Donostia International Physics Center, P. Manuel de Lardizabal 4, 20018 Donostia-San Sebastian, Spain*

<sup>7</sup>*IKERBASQUE, Basque Foundation for Science, Bilbao, Spain*

<sup>8</sup>*Department of Condensed Matter Physics, Weizmann Institute of Science, Rehovot, Israel*

(Dated: June 7, 2024)

Ingap states are commonly observed in semiconductors and are often well characterized by a hydrogenic model within the effective mass approximation. However, when impurities are strong, they significantly perturb all momentum eigenstates, leading to deep-level bound states that reveal the global properties of the unperturbed band structure. In this work, we discover that the topology of band wavefunctions can impose zeros in the impurity-projected Green's function within topological gaps. These zeros can be interpreted as spectral attractors, defining the energy at which ingap states are pinned in the presence of infinitely strong local impurities. Their pinning energy is found by minimizing the level repulsion of band eigenstates onto the ingap state. We refer to these states as *ring states*, marked by a mixed band character and a node at the impurity site, guaranteeing their orthogonality to the bare impurity eigenstates and a weak energy dependence on the impurity strength. We show that the inability to construct symmetric and exponentially localized Wannier functions ensures topological protection of ring states. Linking ring states together, the edge or surface modes can be recovered for any topologically protected phase. Therefore, ring states can also be viewed as building blocks of boundary modes, offering a framework to understand bulk-boundary correspondence.

Topological matter is defined by the existence of Wannier obstructions, which occur when Bloch eigenstates, each with a distinct crystal momentum, cannot be recombined into an orthogonal set of exponentially localized states at specific positions in a unit cell, aligning with the symmetric representation of the site symmetry group [1–7]. In the presence of topological obstructions, symmetric Wannier functions display a polynomial rather than exponential decay around their center. While this nuanced property hasn't been directly measured, current efforts are directed to finding the imposed topological boundary modes [8–12], and bulk electromagnetic responses which are enforced by these obstructions [13–15].

In this work, we show how topological obstructions manifest themselves in *irremovable* states bound to strong local perturbations existing within topological gaps. This phenomenon stands in contrast to the behavior of shallow impurity states, which are mainly influenced by the band edge and well described by effective mass theory [16]. We denote these states *ring states*. They are related to deep-level states in covalent semiconductors but *protected* by the bulk topological invariants. They are non-perturbative and require the summation of the Dyson expansion of the Green's function at all orders in the impurity strength [17–19]. Ring states arise from the mixing of Bloch states across both occupied and unoccupied bands, and their energy within the band gap depends only weakly on the impurity strength. Through this study, we demonstrate that

ingap states bound to strong impurities are not merely incidental but are enforced by bulk topological obstructions. Ring states are topologically protected from symmetric and adiabatic changes in the bulk bands, characterized by their unique spatial avoidance of the defect site and their orthogonality to the bare defect eigenstates.

The widespread occurrence of nontrivial geometry of Bloch bands in the solid state suggests that ring states are not just rare occurrences but a common phenomenon. Notably, deep center defects are common in semiconductors like silicon or diamond [17–20] which are examples of obstructed atomic limits. The topological obstruction in these semiconductors is reflected not only in topologically protected ingap impurity states or surface charge [21, 22] but also in other physical responses, such as unusually large refractive indices [23]. Deep states in these semiconductors can be well understood in the vacancy limit as *dangling bonds* [24]. However, as we prove here these deep states are topologically protected. Non-obstructed semiconductors such as GaAs, which, unlike silicon, have Wannier centers that are not fixed by symmetry to be at the center of the bonds, can also show ingap states with similar features. However, these are not protected by symmetry and could hypothetically be absorbed into the band continuum by symmetric and adiabatic changes in the bulk bands. We reserve the term ring states for those states that are enforced by the symmetry and topology of the bulk. In addition to obstructed atomic limits, ring states appear in topological phases where there is no exponential localization of Wannier orbitals in any symmetric lattice position. That is stable (or fragile)

\* raquel.queiroz@columbia.edu

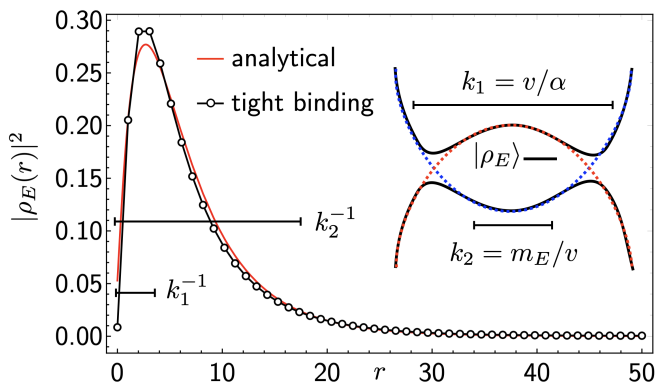


Figure 1. Radial profile of an ingap ring state caused by a local potential in a Chern insulator (18). The ingap state reflects the band inversion in momentum space since the orbital content at short and large distances is inverted. At the core, where the orbital character matches the impurity, the wavefunction is suppressed. It is followed by a maximum and an exponential decay at large distances. Inset: Scheme of a band structure that includes an inversion and energy and length scales that define the resulting ring state. Solution for the ring state located at  $E = -0.184$  with model parameters  $m = -0.2$ ,  $v = 1$  and  $b = 1.5$ .

topological phases. Here, a better physical picture for ring states is that of boundary states compactified into a small, single-site boundary. This is the case of impurity states in topological insulators [25, 26] as well as bound states in the gaps between Landau levels in the quantum Hall regime [27–29]. In these cases, exponentially localized ingap states inherit a mixed band character resembling a small edge mode around the single site defect, see Fig.1. Lastly, ring states can also appear in topological (Dirac or Weyl) semimetals without a band gap due to an ungapped band inversion. In these cases, ring states become long-lived resonances with a small overlap with bulk states, but still characterized by their finite energy in the strong impurity limit, the band character mixing and the orthogonality to the bare impurity eigenstates. Examples are resonant states at vacancies in graphene [30, 31], graphite [32], or Weyl semimetals [33]. In this text we will focus on gapped systems and further discuss semimetals in Ref.[34]. We use the term ring states to encompass all the above cases, defined by their topological protection, orthogonality to the bare defect eigenstates, and energy confined to the bandwidth of the unperturbed Hamiltonian  $\mathcal{H}$ , far smaller than the perturbation  $\mathcal{V}$ .

Discussing topologically protected impurity-bound states on equal footing and highlighting their geometric origin opens up new avenues for using impurities as local probes of band topology, offering a novel method to investigate and understand topological materials. The consistency of these ingap states, largely independent of their local environment, provides valuable insights to applications in optoelectronic devices [35], catalysts [36], and trapping of localized quantum states for quantum information [37] or spectroscopy [38], extending the realm

of these applications to a broader range of materials with topological gaps. Finally, our findings also provide a new perspective on bulk boundary correspondence. The spatially extended nature of ring states allows them to hybridize when in proximity, forming clusters of strong impurities or vacancies. This hybridization leads to the delocalization of ring states, forming boundary modes around the cluster that potentially carry topologically protected currents.

This article is organized as follows: First, we introduce topological obstructions in Sec.IA, and the formalism to find impurity states in Sec.IB. We discuss a simple case of two flat bands with an impurity with varying overlap between bands to illustrate the appearance of the ring states and how they can be interpreted as “antibonding states” between band projected states in Sec.IC. We show in Sec.ID that their pinning energy minimizes the level repulsion exerted by the band states above and below the gap, and associate this energy to the zeros of the impurity projected Green’s function. We generalize our arguments to dispersive bands in Sec.IF and show the spectral and wavefunction evolution of ring states with impurity strength in Sec.IG. We finally discuss the concrete example of ring states in a Chern insulator in Sec.II and their relation with boundary states in Sec.III.

## I. RING STATES

### A. Topological obstructions

We consider a general tight-binding Hamiltonian, constructed from a set of basis states  $|\phi_i^\sigma\rangle$  at lattice sites  $\mathbf{q}_i$  transforming under an irreducible representation  $\sigma$  of the local site symmetry group of  $\mathbf{q}_i$ [39, 40],

$$\mathcal{H} = \sum_{ij,\sigma\tau} h_{ij}^{\sigma\tau} |\phi_i^\sigma\rangle \langle \phi_j^\tau| = \sum_{\mathbf{k}\alpha} \varepsilon_{\alpha\mathbf{k}} |\psi_{\mathbf{k}}^\alpha\rangle \langle \psi_{\mathbf{k}}^\alpha|. \quad (1)$$

The Hamiltonian is diagonalized by Bloch eigenstates with energies  $\varepsilon_{\alpha\mathbf{k}}$ , carrying a band index  $\alpha$  and crystal momentum  $\mathbf{k}$ . We are interested in what a topological obstruction in a band  $\alpha$  can say about the protection of states induced by impurities in gaps between bands. A topological obstruction implies that any set of symmetric Wannier states  $|w_{\mathbf{R}}^\alpha\rangle$  that span a band or connected set of bands  $\alpha$  with projector  $\mathbb{P}^\alpha \equiv \sum_{\mathbf{k}} |\psi_{\mathbf{k}}^\alpha\rangle \langle \psi_{\mathbf{k}}^\alpha| = \sum_{\mathbf{R}} |w_{\mathbf{R}}^\alpha\rangle \langle w_{\mathbf{R}}^\alpha|$  cannot be exponentially localized[2]. As further discussed in App.F this implies that the band does not transform under a band representation[1, 41, 42] and its subspace cannot be adiabatically connected to an atomic subspace  $\mathbb{P}^\sigma \equiv \sum_i |\phi_i^\sigma\rangle \langle \phi_i^\sigma|$ . That is, the overlap between the band subspace and any atomic subspace is necessarily singular, and the overlap matrix introduced in Ref. [43]  $S_{ij}^{\sigma\alpha} = \langle \phi_i^\sigma | \mathbb{P}^\alpha | \phi_j^\sigma \rangle$  has at least one zero eigenstate and therefore zero determinant. The topological obstruction is seen when one attempts to orthogonalize band projected

states transforming under the  $\sigma$  representation [43, 44],

$$|\Upsilon_i^{\sigma\alpha}\rangle \equiv \mathbb{P}^\alpha |\phi_i^\sigma\rangle, \quad (2)$$

which cannot be orthogonalized due to  $\det S^{\sigma\alpha} = 0$ . Note that translation symmetry implies that in the momentum basis  $|\phi_{\mathbf{k}}^\sigma\rangle = \sum_i e^{i\mathbf{k}\cdot\mathbf{q}_i} |\phi_i^\sigma\rangle$ , the overlap matrix is diagonal, with diagonal elements  $s_{\mathbf{k}}^{\sigma\alpha} = |\langle\phi_{\mathbf{k}}^\sigma|\psi_{\mathbf{k}}^\alpha\rangle|^2$ , and therefore the topological obstruction guarantees  $s_{\mathbf{k}}^{\sigma\alpha} = 0$  for at least one point in the Brillouin zone.

In this discussion we have assumed the choice of local basis states forms a complete basis under the action of lattice translations. It follows that if we choose one basis state in particular,  $|\phi_0^\sigma\rangle$ , it cannot be constructed from a single topological band  $\alpha$ , since otherwise, we could use translation symmetry to construct every other basis state  $|\phi_i^\sigma\rangle$  from this subspace resulting in an atomic band. In other words, the projected states  $|\Upsilon_i^{\sigma\alpha}\rangle$  have nonzero norm for bands above and below the topological or obstructed gap. This realization motivates us to consider the effect of a perturbation that affects a single local orbital,

$$\mathcal{V} = v |\phi_0^\sigma\rangle \langle\phi_0^\sigma|, \quad (3)$$

that effectively removes it, or projects it out, from the system at large  $v$ . In the band basis,  $\mathcal{V}$  must affect multiple bands  $\mathcal{V} = v \sum_\alpha |\Upsilon_0^{\sigma\alpha}\rangle \langle\Upsilon_0^{\sigma\alpha}|$  since, as discussed above, the norm  $s_\alpha \equiv \langle\Upsilon_0^{\sigma\alpha}|\Upsilon_0^{\sigma\alpha}\rangle$  is required to be nonzero for at least one band above and below the topological gap, and therefore the perturbation necessarily removes more than one localized state from the band continuum. As we show in the following sections, removing multiple states from the band continuum from a single orbital vacancy implies, by virtue of the conservation of the Hilbert space, the creation of topologically protected bound states in spectral gaps. If the norm  $s_\alpha$  is forced to be nonzero in multiple bands due to a topological obstruction, the ingap state is stable against any symmetric and adiabatic deformation of the clean Hamiltonian  $\mathcal{H}$ . These ingap states, at a finite energy in the limit  $v \rightarrow \infty$  are what we call ring states.

## B. Impurity bound state from the Green's function

We consider a strong local potential in one of the orbitals  $\mathcal{V} = v |\sigma\rangle \langle\sigma|$ , with  $|\sigma\rangle$  shorthand for  $|\phi_0^\sigma\rangle$ , and define the band projected states  $|\Upsilon^\alpha\rangle$  as a shorthand for  $|\Upsilon_0^{\sigma\alpha}\rangle$  with norm  $s_\alpha$ . Adding the symmetric perturbation  $\mathcal{V}$  to  $\mathcal{H}$ , we expect that when  $v \rightarrow \pm\infty$  there is an eigenstate of  $\mathcal{H} + \mathcal{V}$  that coincides with  $|\sigma\rangle$  up to corrections of order  $1/v$ . To see this, we note that the perturbed Hamiltonian has bound state solutions at energies  $E$  outside the band continuum,  $(\mathcal{H} + \mathcal{V})|\varphi_E\rangle = E|\varphi_E\rangle$ , found in terms of the bare Green's function, which takes the form

$$\mathcal{G}(\omega) = \sum_{\alpha\mathbf{k}} \frac{|\psi_{\mathbf{k}}^\alpha\rangle \langle\psi_{\mathbf{k}}^\alpha|}{\omega - \varepsilon_{\alpha\mathbf{k}}}. \quad (4)$$

with  $|\psi_{\mathbf{k}}^\alpha\rangle$  the band eigenstates, and  $\varepsilon_{\alpha\mathbf{k}}$  the band energies. The bound states satisfy

$$|\varphi_E\rangle = \mathcal{G}(E)\mathcal{V}|\varphi_E\rangle, \quad (5)$$

corresponding to poles of the  $T$ -matrix  $\mathcal{T}(\omega) = \mathcal{V}[1 - \mathcal{G}(\omega)\mathcal{V}]^{-1}$  [45, 46], see also App.A. Using our simple impurity form that affects a single orbital  $|\sigma\rangle$ , the only nonzero matrix element of  $\mathcal{T}(\omega)$  which may contain a bound state pole is

$$t^\sigma(\omega) = \langle\sigma|\mathcal{T}(\omega)|\sigma\rangle = \frac{v}{1 - vg^\sigma(\omega)}, \quad (6)$$

where  $g^\sigma(\omega) \equiv \langle\sigma|\mathcal{G}(\omega)|\sigma\rangle$  is the *impurity projected Green's function*. The perturbed Green's function contains a pole at  $g^\sigma(E) = 1/v$ . At the strong impurity limit  $v \rightarrow \pm\infty$ , this pole appears at the energy where  $g^\sigma(\omega)$  is zero. It is convenient to define the impurity projected retarded Green's function

$$g^\sigma(\omega - i0^+) = \mu^\sigma(\omega) - i\pi\nu^\sigma(\omega)$$

where  $\nu^\sigma$  is the projected density of states, positive in the band continuum; and  $\mu^\sigma$  the real part of  $g^\sigma$ . Zeros in  $g^\sigma$  only exist outside the spectrum of  $\mathcal{H}$  where both  $\nu^\sigma = 0$  and  $\mu^\sigma = 0$ . Since as long as  $|\sigma\rangle$  belongs to the Hilbert space of  $\mathcal{H}$  at energies far above or below the unperturbed spectrum,  $g^\sigma \sim 1/\omega$ , it is always guaranteed that there is one and only one bound state at a large energy  $E \sim v$  outside the spectrum of  $\mathcal{H}$ . In fact, this is a simple consequence of Weyl's inequalities [47] which guarantees that the number of eigenstates of  $\mathcal{H} + \mathcal{V}$  outside the spectral width of  $\mathcal{H}$  is at most the rank of  $\mathcal{V}$ , which we chose to be one for simplicity. It follows that if any other bound state solution of (5) appearing from  $g^\sigma = 0$  must be confined to the gap between bands. As we will see in the next sections, such states can be required to exist from topological obstructions.

## C. Exact bound state solution for two flat bands

Let us first consider the simple yet enlightening case of two non-degenerate flat bands,  $\alpha = 1, 2$ . Without loss of generality, they are located at energies  $\varepsilon_1 = 0$  and  $\varepsilon_2 = \Delta$ . The tight-binding Hilbert space in (1) contains two orthogonal basis orbitals  $\sigma = 1, 2$  per unit cell. We define the band projected states  $|\Upsilon^1\rangle \equiv \mathbb{P}^1|\sigma\rangle$  of norm  $s_1$  and  $|\Upsilon^2\rangle \equiv \mathbb{P}^2|\sigma\rangle$  of norm  $s_2$ , satisfying  $s_1 + s_2 = 1$ . The difference  $\delta s = s_1 - s_2$  characterizes the relative overlap of the impurity  $\mathcal{V}$  with both bands.

Introducing the bare flat band Green's function

$$\mathcal{G}(\omega) = \sum_{\alpha} \frac{\mathbb{P}^\alpha}{\omega - \varepsilon_\alpha}. \quad (7)$$

in the bound state equality (5), we find the general form for a bound state in the flat band limit

$$|\varphi_E\rangle = \sum_{\alpha} \frac{v\lambda_E}{E - \varepsilon_\alpha} |\Upsilon^\alpha\rangle, \quad (8)$$

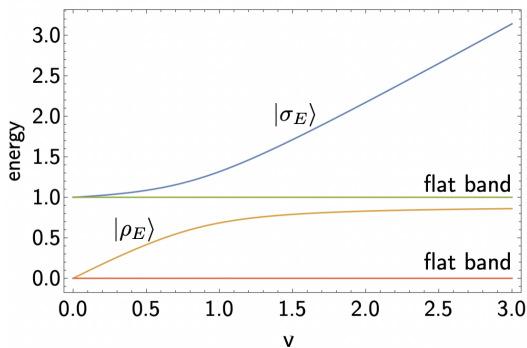


Figure 2. Evolution of the bound state energies for two flat bands separated by a gap  $\Delta = 1$ , caused by an impurity that overlaps with both bands, with a relative overlap of  $\delta s = 0.9$ . At  $v \rightarrow \infty$ , the pinning energy  $E_\infty$  of the ingap bound state  $|\rho\rangle$  reflects how much the impurity state  $|\sigma\rangle$ , overlaps with the bands above and below the gap, therefore reflecting the orbital content of the unperturbed bands.

with  $\lambda_E \equiv \langle \sigma | \varphi_E \rangle$  a scalar reflecting the overlap between the bound state  $|\psi_E\rangle$  and the affected orbital, or bare impurity eigenstate,  $|\sigma\rangle$ . For large  $v$ , we consider the only two possible bound states. One, with a large overlap with  $|\sigma\rangle$  which we call  $|\sigma_E\rangle$ , with  $\lambda_E \sim 1$ . The energy of this bound state is  $E \sim v$  and exists independently of the details of the Hamiltonian  $\mathcal{H}$ . A second solution  $|\rho_E\rangle$  exists exclusively in multi-band Hamiltonians when  $v\lambda_E$  remains finite as  $v \rightarrow \infty$  by acquiring a vanishingly small overlap  $\lambda_E \rightarrow 0$  with the bare impurity eigenstates  $|\sigma\rangle$ . In other words, to guarantee its finite energy  $E$ , the ingap state avoids the impurity by the orthogonality of its wavefunction. Since  $|\rho_E\rangle$  transforms under the same symmetry representation as the impurity eigenstate  $|\sigma\rangle$ , this orthogonality can only be assured by spatially avoiding the bare impurity eigenstate  $|\sigma\rangle$ , forming a node at the impurity site. That is, the state  $|\rho_E\rangle$  forms a *ring* around the impurity.

Now we show that the energy of the state  $|\rho_E\rangle$  in the large  $v$  limit is determined by the unperturbed Hamiltonian  $\mathcal{H}$  and the affected state up to order  $O(1/v)$ , becoming largely independent of the magnitude of the impurity  $v$  in the limit  $v \rightarrow \infty$ . Specifically, in our example, the energies of the bound states are obtained by taking the inner product  $\langle \sigma | \varphi_E \rangle$  in (8) and solving for the energy  $E$ . This leads to two solutions, see App.B for further details,

$$E_{\pm} = \frac{1}{2}(\Delta + v \pm \sqrt{\Delta^2 + 2v\delta s\Delta + v^2}), \quad (9)$$

for  $\delta s = s_1 - s_2$ , plotted in Fig.2. We consider without loss of generality  $v > 0$  and  $s_1 > s_2$ . In this case,  $E_+ \sim v + \Delta(1 - \delta s)/2$  and  $E_- \sim \Delta(1 + \delta s)/2$ , to first order in  $1/v$ . As long as  $|\delta s| \neq 1$ , there are *two* solutions that deviate from the unperturbed band energies. At infinite  $v$ , the  $|\rho\rangle$  state remains in the gap, at a distance  $\Delta s_1$  from the bottom band and  $\Delta s_2$  from the top band.

As we explicitly demonstrate in App.A, the wavefunction of the  $|\rho_E\rangle$  state solution up to correction of order

$1/v^2$  is given by

$$|\rho_E\rangle \sim [1 + \frac{\Delta s_2}{v}] \sqrt{\frac{s_2}{s_1}} |\Upsilon^1\rangle - [1 + \frac{\Delta s_1}{v}] \sqrt{\frac{s_1}{s_2}} |\Upsilon^2\rangle. \quad (10)$$

This solution can only exist if both projected states  $|\Upsilon^\alpha\rangle$  can be normalized. The limiting form of the ingap state is independent of  $v$ ,

$$|\rho_E\rangle \rightarrow |\rho\rangle = \sqrt{s_2/s_1} |\Upsilon^1\rangle - \sqrt{s_1/s_2} |\Upsilon^2\rangle. \quad (11)$$

This asymptotic form can be interpreted as an “antibonding state” between the two projected states  $|\Upsilon^\alpha\rangle$  removed from the bands above and below the gap by the impurity  $\mathcal{V}$ , orthogonal to the eigenstate of the bare impurity  $\mathcal{V}$  or “bonding state”  $|\sigma\rangle = |\Upsilon^1\rangle + |\Upsilon^2\rangle$ . Both states are normalized. The overlap between the ring state and the original unperturbed bands is opposed to the overlap of the impurity state. That is  $\langle \rho | \mathbb{P}^1 | \rho \rangle = s_2$  and  $\langle \rho | \mathbb{P}^2 | \rho \rangle = s_1$ .

Note that at this stage we have not yet related the state  $|\rho_E\rangle$  to the topology of the band. A topological obstruction implies that  $s_\alpha \neq 1$  if the bands are not adiabatically equivalent to the atomic limit induced by the orbital  $|\sigma\rangle$  at the impurity position  $\mathbf{q}_0$ , which uniquely determines the band representation[48]. In the flat band limit, we have shown here that an ingap state exists as long as  $s^\alpha \neq 1$  for all bands. This encompasses many instances of ingap states which are not topologically protected. However, *the ring state will exist and be topologically protected if neither band above or below the gap transforms under the band representation defined by  $\mathcal{V}$* . If there is a strong topological obstruction, where the bands below the topological gap do not transform under *any* band representation of the space group, and the bands do not admit symmetric and exponentially localized Wannier functions, then a ring state is *always* expected. If the bands transform under a band representation but not the one defined by  $|\sigma\rangle$  and  $\mathbf{q}_0$ , the ring state is also protected. Note that if we assume that the impurity site coincides with an atomic site, all obstructed atomic, fragile, and stable topological phases host topologically protected ring states. If we allow  $\mathcal{V}$  to be centered away from atomic sites, such as affecting bonds, then only stable topological phases will necessitate ingap ring states. If no topological obstruction prevents it, the state  $|\sigma\rangle$  can belong either to the top or bottom bands. Choosing in this case  $\delta s = 1$  we find by solving Eq.(9) that  $|\sigma_E\rangle$  is located at  $E_+ = v$ , while  $E_- = \Delta$  is the band energy, implying that there is no ingap solution.

Beyond the flat band limit, we find that the necessity of the ring state remains true, while topologically unprotected ingap states can disappear when the perfect overlap condition is relaxed. To appreciate this fact, we look in the following sections at the structure of the unperturbed Green’s function which leads to the protection of ingap states.

### D. Level repulsion interpretation

In the previous section, we have seen that the ring state consists of a linear combination of impurity projected states  $|\Upsilon^\alpha\rangle$  from bands above and below the gap. As it is apparent in Fig.2, the ring state may be forced to remain in the gap at large  $v$  from the level repulsion exerted by the perturbed band states and prevented from piercing through the band and becoming perfectly localized at the impurity location  $\mathbf{q}_0$  with energy  $E \sim v$ . This observation can be made precise by referring to the structure of the impurity projected Green's function  $g^\sigma$ . The necessity of an ingap ring state follows from the necessity of ingap zeroes of  $g^\sigma$ . It follows from Eq.(4), that in the flat band limit  $g^\sigma(\omega) = \sum_\alpha s_\alpha/(\omega - \varepsilon_\alpha)$ . It contains a pole at every (flat) band energy provided  $s_\alpha \neq 0$ . Naturally, in the topological case where both poles have a nonzero residue,  $g^\sigma$  must change sign for some ingap energy  $\varepsilon_1 < E_\infty < \varepsilon_2$ .

It is enlightening to consider the evolution of the bound state energy  $E(v)$  with the perturbation strength  $v$ ,  $\mathcal{H}(v) = \mathcal{H} + v|\sigma\rangle\langle\sigma|$ . As we show in App.D, second-order perturbation theory requires the second derivative of the bound state energy with respect to  $v$  to satisfy a Newton's law

$$\partial_v^2 E = 2\lambda_E^2 \mu^\sigma(E). \quad (12)$$

with  $\mu^\sigma(\omega)$  the real part of the impurity projected retarded Green's function and  $\lambda_E$  the overlap between the state at energy  $E$  and the bare impurity eigenstate  $|\sigma\rangle$ . That is,  $\mu^\sigma$  can be interpreted as a *force* on a state of energy  $E$  exerted by all other eigenstates due to their overlap with the bound state through the impurity. Notably, the sign of  $\mu^\sigma$  indicates the sign of this force, and zeroes of  $\mu^\sigma$  are fixed points of Eq.(12).

Eq.(12) can be interpreted as follows: Consider a small potential affecting a particular site ( $v > 0$ ) as shown in Fig.2. In the flat band limit, there are only isolated poles in  $g^\sigma$  at the flat band energies, and away from it the Green's function is real, negative below the band and positive above. We can write  $\mu^\sigma(E) \sim g^\mu(E)$  for  $E \neq \varepsilon_\alpha$ . Since  $\mu^\sigma$  is positive just above every band with  $s_\alpha \neq 0$ , it will pull a state from both bands, moving it to higher energies as  $v$  increases until the states reach energies at which  $\mu^\sigma(E) = 0$ . The state from the top band will be pushed to  $E_\infty = +\infty$  since asymptotically  $\mu^\sigma(E) = 1/E$ . On the other hand, the state removed from the bottom band moves towards the upper band until it starts feeling its repulsion, which contributes a negative  $\mu^\sigma$ . When the repulsion between the two bands is balanced  $\mu^\sigma(E_\infty) = 0$ , and the ingap state assumes its final energy. At large  $v$  this energy reflects solely the structure of the bare Green's function, namely the overlap between the unperturbed bands with the impurity eigenstate.

Since  $\mu^\sigma(\omega)$  decreases monotonically outside the spectrum of  $\mathcal{H}$ , the slope of  $\mu^\sigma$  is negative  $\partial_\omega \mu^\sigma < 0$  for any ingap zero. The negative slope implies that the force is positive for energies below the zero and negative for energies above, and therefore these zeroes are characterized by

a restoring force that pushes the bound state to a pinning energy  $E_\infty$  in the strong impurity limit. We denote these zeroes as *spectral attractors*, and  $E_\infty$  corresponds to the energy that minimizes the level repulsion between the ingap state and the bands above and below the gap. On the other hand, if a zero has a positive slope  $\partial_\omega \mu^\sigma > 0$ , it corresponds to an unstable fixed point or a *spectral repeller*. It denotes an energy with a destabilizing force pushing states away from it. Such points can only exist within a band continuum. From the pinning energy of the ring state, which in Fig.2 corresponds to  $E_\infty = 0.95\Delta$ , we can read that the state  $|\sigma\rangle$  is 95% supported in the lower band, and 5% in the upper band, and vice versa for the  $|\rho\rangle$  state, which will have a band character close to the top band. The same state could have been obtained by putting a local negative potential, which would quickly remove a state from the top band and create the same ring state.

### E. Necessity of ring states in topological gaps

Now, we prove that the ring state is a topologically protected ingap state if the Bloch bands  $\mathbb{P}^\alpha$  are not adiabatically connected to the atomic limit defined by the state  $|\sigma\rangle$ . To do so, we ask if the ring state  $|\rho\rangle$  can be absorbed into a perturbed band  $\tilde{\mathbb{P}}^\alpha$  formed by the extended scattering eigenstates in the presence of the impurity  $\mathcal{V}$ . That is, we ask if it is possible to remove the ingap state by adiabatic changes in the unperturbed Hamiltonian  $\mathcal{H}$ . Completeness ensures that

$$\sum_\alpha \tilde{\mathbb{P}}^\alpha + |\sigma\rangle\langle\sigma| + |\rho\rangle\langle\rho| = \sum_\alpha \mathbb{P}^\alpha = \mathbb{1}. \quad (13)$$

One can immediately see that the overlap  $\langle\sigma|\tilde{\mathbb{P}}^\alpha|\sigma\rangle = 0$  as well as  $\langle\sigma|\rho\rangle = 0$ , and the combined subspace  $\tilde{\mathbb{P}}^\alpha + |\rho\rangle\langle\rho|$  has no overlap with the state  $|\sigma\rangle$ . On the other hand,  $\langle\sigma|\mathbb{P}^\alpha|\sigma\rangle > 0$  is protected by the topological obstruction of the band. If we were to assume it is possible to absorb  $|\rho\rangle$  into one of the perturbed bands, that is, to bring this state into the band continuum and perform a symmetric and unitary transformation on the band states such that  $\tilde{\mathbb{P}}^1 + |\rho\rangle\langle\rho| \rightarrow \mathbb{P}^1$ , then it would necessarily be the case that under the same transformation  $\tilde{\mathbb{P}}^2 + |\sigma\rangle\langle\sigma| \rightarrow \mathbb{P}^2$  since the Hilbert space must remain the same under this transformation. That is, such a unitary transformation would take the unperturbed band  $\alpha = 2$  to an atomic limit spanned by the  $|\phi_i^\sigma\rangle$  orbitals, which is *incompatible* with the assumption of a topological obstruction. This argument requires only that the two band subspaces remain well-defined through this transformation. That is, the gap between  $\tilde{\mathbb{P}}^\alpha$  is preserved. Importantly, it does not require the bands to be flat.

## F. Ring states in dispersive bands

In the flat band example we have seen by explicit computation that the ring state wavefunctions are orthogonal to the impurity eigenstates, containing nonvanishing projections of multiple unperturbed bands; and their limiting energy is determined by the zeroes of the real part of the unperturbed impurity projected Green's function  $\mu^\sigma$ . We have interpreted these zeroes as finite fixed energy points of the energy spectrum in the strong impurity limit. We have seen that if the gap is topological, the ring state cannot be absorbed into the band continuum, which is equivalent to say that the zero in  $\mu^\sigma$  is irremovable. We now expand this argument to the general case of dispersive bands.

First, let us note that an ingap zero in  $\mu^\sigma$  always implies there is an ingap bound state in the strong impurity limit. Eq.12 holds true for flat or dispersive bands, and the intuition built in the previous section can be applied in the current case: this ingap state is prevented from entering the bands above or below the topological gap by level repulsion imposed by  $\mathcal{V}$ . Moreover, the argument in Sec.IE still holds. There is necessarily an obstruction to adiabatically deform the perturbed bands together with the ring state to the unperturbed bands when there is a topological obstruction. However, unlike in the flat band limit, the requirement for the existence of an ingap state is more stringent: Even when the overlap  $s^\alpha$  is non-zero in bands above and below the gap, a ring state (ingap attractor, zero of  $\mu^\sigma$  with negative slope) is only guaranteed if a repeller (zero of  $\mu^\sigma$  with positive slope) exists in bands above and below the gap. To appreciate this fact we consider the qualitative features that distinguish trivial from topological bands in the impurity projected retarded Green's function  $g^\sigma(\omega - i0^+) = \mu^\sigma(\omega) - i\pi\nu^\sigma(\omega)$  where  $\nu^\sigma$  is the projected density of states, positive in the band continuum; and  $\mu^\sigma$  was previously identified as a force in the presence of the onsite perturbation  $\mathcal{V}$ . A Hilbert transformation relates the two quantities.

Ingap ring state solutions are possible when  $g^\sigma$  (or equivalently its real part  $\mu^\sigma$  since in the gap  $\nu^\sigma = 0$ ) contains an ingap zero. Projecting (4) onto the impurity eigenstate  $|\sigma\rangle$  we find

$$g^\sigma(\omega) = \frac{1}{N} \sum_{\alpha, \mathbf{k}} \frac{s_{\alpha\mathbf{k}}^\sigma}{\omega - \varepsilon_{\alpha\mathbf{k}}}, \quad (14)$$

with poles at the band energies  $\varepsilon_{\alpha\mathbf{k}}$ , weighted by the overlap  $s_{\alpha\mathbf{k}}^\sigma \equiv |\langle \phi_{\mathbf{k}}^\sigma | \psi_{\alpha\mathbf{k}} \rangle|^2$ , satisfying  $0 \leq s_{\alpha\mathbf{k}}^\sigma \leq 1$ , and the total overlap is  $s_\alpha = 1/N \sum_{\mathbf{k}} s_{\alpha\mathbf{k}}^\sigma$ . For flat topological bands, we have seen that (14) has a change of sign across multiple bands, and therefore it has a zero at some ingap energy  $E_\infty$ . On the other hand, this zero is absent (or removable) in the trivial case.

In the case of dispersive bands  $g^\sigma$  does not diverge necessarily above and below the bands. Therefore, our focus is on the phase evolution of  $g^\sigma(\omega - i0^+)$ . Phase jumps of  $\pi$  accompany zeroes of  $\mu^\sigma$ , and therefore detect

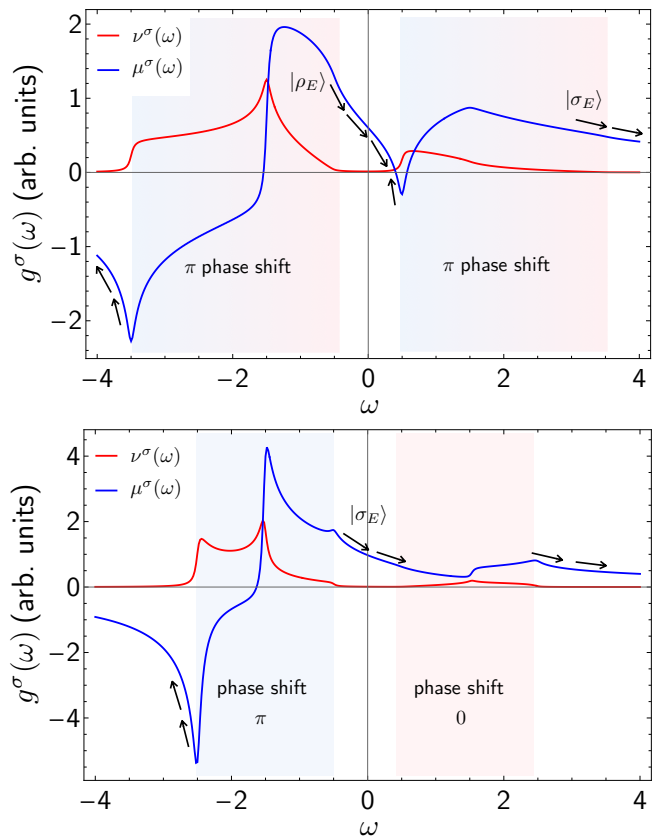


Figure 3. Impurity projected Green's function  $g^\sigma(\omega) = \mu^\sigma(\omega) - i\pi\nu^\sigma(\omega)$  for an orbital vacancy in a Chern insulator (18) in the topological (top panel) and trivial (bottom panel) phases. The Wannier obstruction is reflected in an irremovable  $\pi$  phase shift across *both* topological bands, and a topologically robust zero of  $\mu^\sigma(\omega)$  in the band gap. This zero is a finite energy spectral attractor that binds a state in the strong impurity limit. The energy of the ring state  $|\rho_E\rangle$  flows towards a fixed energy  $E_\infty$  that minimizes the level repulsion from the valence and conduction bands, and its wavefunction to a state  $|\rho\rangle$  orthogonal to  $|\sigma\rangle$ . On the other hand, the trivial state  $|\sigma_E\rangle$  is taken to infinite energy in the same limit, adiabatically connected to the impurity eigenstate  $|\sigma\rangle$ . We consider  $v = 1$  and  $b = 1$ , and  $m = -0.5$  for the topological and  $m = +0.5$  in the trivial case.

the existence of spectral fixed points. This is best seen in the change in the local density of states  $\delta\nu^\sigma$  induced by  $\mathcal{V}$ . At any impurity strength,  $\delta\nu^\sigma$  is given by

$$\delta\nu^\sigma(\omega) = -\frac{1}{\pi} \partial_\omega \eta^\sigma(\omega), \quad (15)$$

where the phase shift  $\eta^\sigma(\omega) \equiv \arg t^\sigma(\omega - i0^+)$  is obtained from the T-matrix, whose nonzero eigenvalues  $t^\sigma$  are given in Eq.(6). The phase shift approaches  $\eta^\sigma \sim \arg g^\sigma(\omega - i0^+)$  at  $v \rightarrow \pm\infty$ . See App.A for further details. It follows that the total number of states removed from a band  $\alpha$

can be written as

$$N^\alpha = \int_{\varepsilon_{\min}^\alpha}^{\varepsilon_{\max}^\alpha} \frac{1}{\pi} \partial_\omega \eta^\sigma(\omega) d\omega, \quad (16)$$

for  $\varepsilon_{\min/\max}^\alpha$  the extremal energies of the band. Since we chose for simplicity  $\mathcal{V}$  of rank 1,  $N^\alpha = 0, 1$  depending on whether there is a 0 or a  $\pi$  phase shift across the band, respectively. More generally, at any rank of  $\mathcal{V}$ , the number of removed states  $N^\alpha$  and ring states  $N_{\text{ring}}$  satisfies a Friedel sum rule,

$$\sum_\alpha N^\alpha = N_{\text{ring}} + \text{rk } \mathcal{V}, \quad (17)$$

since the rank  $\text{rk } \mathcal{V}$  determines the number of states projected out of low energies by  $\mathcal{V}$ . That is, the number of bound states with energies of order  $v$ . The total number of ring states added to the number of high-energy states projected out by  $\mathcal{V}$  must equal the number of states removed from the band continuum since the Hilbert space is kept at a constant size.

Let us now illustrate how the phase shifts in the Green's function appear from band inversions. Let us consider a two-dimensional insulator formed by two local orbitals  $\sigma = s, p$  forming two bands, one transforming under an  $s$  band representation (valence) and a  $p$  band representation (conduction). By inverting the band character between the top of the valence band and the bottom of the conduction band, the insulator enters a Chern insulating phase. Note that here we describe the transition qualitatively and leave the quantitative analysis to Sec. II. The impurity projected Green's function is shown in Fig. 3. Focusing on one orbital projection, say  $\sigma$  is an  $s$  orbital, we expect, in the trivial case, both the top and bottom band edges of the valence band to be of  $s$  type, leading to a step function in  $\nu^s$  at both ends of the valence band. Correspondingly, its Hilbert transform  $\mu^s$  will show a divergence at both band edges with opposite signs, leading to a  $\pi$  phase shift across the band. On the other hand, the conduction band has a  $p$  character on the band edges, and  $\mu^\sigma$  is finite and positive below and above the top band, and therefore there is a zero phase shift across the conduction band. This is compatible with an adiabatic deformation of both bands into the atomic limit, in which  $\nu^s = 0$  in the conduction band. After the band inversion, the band edge shifts across the gap from one band to another (top panel), and the divergence in  $\mu^\sigma$  appears at the bottom of the conduction band rather than the top of the valence band. This imposes a  $\pi$  phase shift across both the valence *and* conduction bands, unlike in the trivial phase. The topological phase transition is characterized by creating two additional zeros of  $\mu^\sigma$ , an attractor in the gap, and a repeller in the conduction band. This means that a strong  $s$ -like impurity will now remove a state from the conduction band, as we expected from the topological case.

In order to show that the zero in  $\mu^\sigma$  is topologically protected, let us consider deformations in the dispersion

of the bands and, therefore, deformations in the projected density of states  $\nu^\sigma$ . First, we notice that if the bands are topological  $\nu^\sigma$  cannot be made to vanish identically in either band since it would imply there exists an  $s$  orbital compactly localized in a single unit cell in the subspace of the other band, which is a contradiction.

Given this constraint and the fact that  $\mu^\sigma$  and  $\nu^\sigma$  are related by a Hilbert transform, we can show that the attractor in the gap and the repeller in the band cannot annihilate each other without closing the bulk gap. Consider that at the edge of the top band, where we want to annihilate one repeller and one attractor at the band edge, that is two zeros of  $\mu^\sigma$  of the opposite slope at each side of the band edge, and the projected density of states  $\nu^\sigma$  is nondivergent [49], growing with a power law  $\nu^\sigma(\omega) \sim \omega^\gamma$  until a cutoff energy  $W$ . The two zeros can annihilate each other if and only if the condition  $\mu^\sigma = \partial_\omega \mu^\sigma = 0$  can be satisfied. We find this is not possible without involving remote bands. Namely, if  $\gamma = 0$  the slope  $\partial_\omega \mu^\sigma \sim 1/\omega$  at the band edge. For  $\gamma = 1$  the slope diverges logarithmically  $\partial_\omega \mu^\sigma \sim \log(1 - W/\omega)$  and finally for any power  $\gamma > 2$ ,  $\partial_\omega \mu^\sigma \sim -\gamma W^\gamma / (\gamma - 1)$ . That is, the slope of  $\mu^\sigma$  when approaching the band edge is *strictly negative*, and can never vanish unless the projected density of states  $\nu^\sigma$  vanishes itself.

Notice that when  $\nu^\sigma$  grows slowly with energy  $\omega$ , which occurs for example when the minimum of the band is not at the band inversion point, it is possible to find the attractive zero of  $\mu^\sigma$  overlapping with the band continuum where  $\nu^\sigma \neq 0$ , which will lead to a weak hybridization with the delocalized band eigenstates. This implies that the ring state becomes a long-lived resonance with a lifetime  $\Gamma^\sigma = \nu^\sigma / \partial_\omega \mu^\sigma$ . This scenario is particularly important when the band inversion occurs at a larger energy than the direct spectral gap, such as in Dirac semimetals or semimetals with indirect gaps, which is further discussed in Ref. [34].

### G. Spectral evolution of ring states

We now describe the evolution of the energy of the ring states  $|\rho_E\rangle$  which converges to a state  $|\rho\rangle$  orthogonal to the impurity eigenstate  $|\sigma\rangle$ , and contrast it with a regular impurity state  $|\sigma_E\rangle$ , adiabatically connected to  $|\sigma\rangle$ , as a function of the impurity strength  $v$ . From (6), we know the energy of any bound state is determined by the solutions of  $\mu^\sigma(E) = 1/v$ . When  $v \rightarrow \pm\infty$ , a state at energy of order  $v$  is created, corresponding to the asymptotic behavior of  $\mu^\sigma \sim 1/\omega$  far outside the spectrum of  $\mathcal{H}$ . The ring state, in contrast, is positioned at an energy region in which  $\mu^\sigma(\omega)$  crosses zero linearly. It is illuminating to plot the evolution of the energy as a function of  $v^{-1}$  rather than  $v$  to show the topological nature of the ring state. Namely, we look at a compact loop in the impurity strength (identifying  $v = +\infty$  and  $v = -\infty$ ) as introduced in Ref. [33], and see that the ring state is transferred between bands and across the gap,

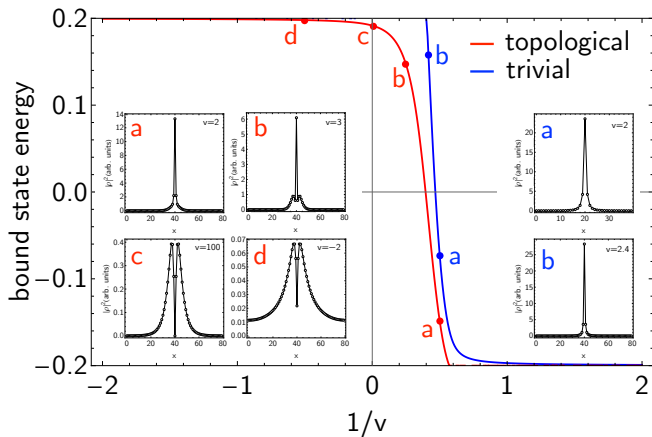


Figure 4. Ingap spectrum of  $\mathcal{H} + \mathcal{V}$  as a function of  $1/v$  for the topological ( $m = -0.2$ ) and trivial ( $m = +0.2$ ) phases of a Chern insulator on a square lattice with  $v = 1$  and  $b = 1.5$ , which approximates well the continuum limit (18). In the trivial case, the impurity state becomes sharper with increasing  $v$ , crossing through the bulk gap and upper bands. In the topological case the state remains in the gap by suppressing its weight at the impurity's core. The same impurity  $\mathcal{V}$  leads to drastically distinct bound states depending on the global geometry of the hosting system's bands. The formation of ring states is expected for *any* symmetric local perturbation in topological bands, while in trivial bands there is always a choice of  $\mathcal{V}$  for which a ring state is not formed.

effectively being “pumped” between partner bands. That is, bands whose combined subspace contains the state  $|\sigma\rangle$ . In the topological phase with a  $\pi$  phase shift across valence and conduction bands, when  $v^{-1} \rightarrow +\infty$  the impurity is weak and repulsive and the ingap state appears above the top of the conduction band. At  $v^{-1} \rightarrow -\infty$  the impurity is weak and attractive, and the ingap state is just below the top of the valence band. Since  $\mu^\sigma$  is continuous in the gap, the evolution of the energy as a function of  $v^{-1}$  is continuous, including when  $v^{-1}$  changes sign. The ingap state then crosses the topological gap, moving smoothly from the valence to the conduction band as  $v^{-1}$  evolves from  $+\infty$  to  $-\infty$ , developing a node at the impurity site to remain at a finite energy across  $v^{-1} = 0$  see Fig.4. On the other hand, in a trivial phase with the  $\pi$  phase in the valence band, the state removed from the valence band gets more localized as  $v$  is increased and pierces through the conduction band and out of the band gap. In this case, a weak attractive potential does not lead to an ingap state.

## II. RING STATE OF A CHERN INSULATOR

We now illustrate the ring state in the solvable case of an  $s$ - $p$  band inversion in a Chern insulator on a (spinless) square lattice. Close to a topological phase transition, the band is well described by a continuum isotropic two-band model  $\mathcal{H} = \sum_{\mathbf{k}} c_{\mathbf{k}}^\dagger h(\mathbf{k}) c_{\mathbf{k}}$  where  $c_{\mathbf{k}\sigma}^\dagger$  creates a basis state

$|\phi_{\mathbf{k}}^\sigma\rangle$  with an orbital character  $\sigma = s, p$  eigenvalue of  $\sigma_z$ , and the Hamiltonian in Fourier space is given by

$$h(\mathbf{k}) = (m + bk^2)\sigma_z - vk_x\sigma_x - vk_y\sigma_y. \quad (18)$$

We define  $m_E^2 = m^2 - E^2$  and introduce two momentum scales  $k_1 = m_E/v$  and  $k_2 = v/b$ , which determine the long-distance and short-distance behavior of  $h(\mathbf{k})$ . For  $m < 0$ , and  $b, v > 0$ ,  $h(\mathbf{k})$  is in a topological phase.

Let us consider the effect of an impurity of  $s$  character. First, we notice that at  $k < k_1$ , the low energy band is dominated by the  $p$  character, while for  $k > k_2$ , the band has  $s$  character, coinciding with the impurity. A localized solution at finite energy composed of Bloch states from the inverted bands will necessarily behave differently at different length scales. Using  $\mathbf{r} = re^{i\varphi}$ , we find the diagonal elements of the Green's function in orbital space is given by the matrix elements between local basis states  $|\phi_{\mathbf{r}}^\sigma\rangle$ ,  $g^\sigma(\omega; \mathbf{r}) = \langle \phi_{\mathbf{r}}^\sigma | \mathcal{G}(\omega) | \phi_0^\sigma \rangle$  are  $\varphi$  independent and given by

$$g^\sigma(\omega; \mathbf{r}) = \sum_{\alpha=1,2} (-1)^\alpha \frac{\omega + \langle \sigma_z \rangle_\sigma (m - bk_\alpha^2)}{\pi b^2 (k_2^2 - k_1^2)} K_0(k_\alpha r) \quad (19)$$

where  $K_0$  is a modified Bessel function of the second kind and  $\langle \sigma_z \rangle_\sigma$  the eigenvalue of  $\sigma_z$  in the state  $|\sigma\rangle$ ,  $\langle \sigma_z \rangle_\sigma = \pm 1$  for  $s$  and  $p$ , respectively. The radial profile of the ring state wavefunction can be computed combining Eqs.(8) and (19),  $\langle r | \rho_E \rangle = g^\sigma(E; r)$  with  $E$  the solution of  $\text{re } g^\sigma(E; r=0) = 1/v$ , and it is shown in Fig.1. The angular ( $\varphi$ ) dependence of the ring state appears from the off-diagonal terms and orbital mixing terms in the Green's function  $\langle \phi_{\mathbf{r}}^\sigma | \mathcal{G}(\omega) | \phi_0^\sigma \rangle$  and are unimportant for determining whether the ring state exists. However, they are consequential for their full wavefunction, on which the details are left to further studies.

Here, we focus on how the competition between the two length scales that appear in the Hamiltonian (18), the short distance  $k_1^{-1}$ , below which the sign of  $m$  dictates the orbital character (here, the eigenvalue of  $\sigma_z$ ), and  $k_2^{-1}$  above which the orbital character is determined by the sign of  $b$ . These two scales are reflected in which term in (19) dominates, resulting in the non-monotonic behavior of  $|\rho_E(r)|^2$ . The band inversion is particularly apparent in the intermediate region  $k_1^{-1} < r < k_2^{-1}$ , where the ring state shows a logarithmic decay due to the admixture of orbital character in the bands in the momentum window  $k_2 < k < k_1$ , see Fig.1.

From Eq.(19), we see that ring states are large,  $r_2 \gg a$ , when their energy approaches the band edge and the mass gap is small, and have a pronounced core  $r_1 > a$  when the band inversion takes only a small portion of the Brillouin zone. If the band inversion is large,  $k_1 \sim \pi/a$ , then the core is narrow  $r_1 \sim 2a$ . Note that the  $k^2$  term plays a crucial role in our discussion, implying that the regularization of the theory at large energies is *required* to properly define the ring state and the topological phase. When this term is absent, we can conclude that  $\mu^\sigma$  monotonically increases with  $\omega$ , and in particular it is enforced to have



a repeller at  $\omega = \pm\infty$ , implying that the bound state comes from infinite energy, a fingerprint of an anomalous theory that does not conserve the number of states. The existence of a ring state can only be guaranteed for a well-regularized theory with a well-defined topological obstruction.

### III. BEYOND RANK 1 PERTURBATIONS

The power of the present analysis is that it describes in equal footing topologically stable ingap states in any band structure, and therefore it can straightforwardly be generalized to any perturbations  $\mathcal{V}$  affecting a tight-binding Hamiltonians, from topological insulators to crystalline topological phases. The natural first generalization of our discussion is to consider perturbations of higher rank than one, which we now briefly discuss.

Let us consider, for example, four-band models of topological insulators such as the Bernevig-Hughes-Zhang [50] or Kane-Mele models [8], both defined and characterized in App.E. Considering a perturbation  $\mathcal{V}$  that preserves time-reversal symmetry, its rank will be  $\text{rk } \mathcal{V} = 2$ , corresponding to a local potential that affects a Kramers pair of a given orbital quantum number. In this case, we can carry out our analysis for each spin sector and find a Kramer's pair of degenerate ring states at some pinning energy  $E_\infty$  within the gap determined by the clean Hamiltonian. That is, the (ingap) zero eigenvalues of  $\mathcal{G}(\omega)$  projected into the two-dimensional eigenspace of  $\mathcal{V}$ . A fragile topological phase [7, 51] protected for example by the combination of time-reversal and an inplane inversion  $C_2\mathcal{T}$  must also bind ring states at any local  $C_2\mathcal{T}$  symmetric perturbation at a lattice site. The simplest example of a symmetric perturbation, irrespective of the system in study, is a lattice vacancy, the absence of all orbitals at one lattice site  $\mathbf{q}_0$ , and therefore, ring states bound to vacancies can be a good indicator of topological obstructions.

Expanding our argument to potentials that affect multiple sites,  $\mathcal{V} = \sum_i v |\mathbf{q}_i\rangle \langle \mathbf{q}_i|$ , more ingap states can be created, however their exact number is not topologically protected. A limit worth considering is combining multiple vacancies to create an edge. Let us consider that momentum along the edge is a good quantum number, say  $k_y$ . Therefore, we can work in the Fourier basis along the  $y$  direction and decompose the edge perturbation as  $\mathcal{V} = \sum_{k\sigma} v |\phi_{x_0, k_y}^\sigma\rangle \langle \phi_{x_0, k_y}^\sigma|$  with  $|\phi_{x, k_y}^\sigma\rangle = \sum_y e^{iyk_y} |\phi_{x, y}^\sigma\rangle$ . Since also  $\mathcal{G}(\omega)$  is diagonal in momentum space, the  $T$ -matrix is diagonalized by  $k_y$ . Ingap states are expected at the condition  $\det(\mathcal{G}(E)\mathcal{V} - 1) = 0$ , as it is discussed in Ref. [25]. Ingap zeros of  $\mathcal{G}(\omega; k_y)$  will exist only for a subset of momenta in the edge Brillouin zone up to the momenta at which the boundary states merge into bulk states. Note the region in  $k_y$  for which edge bound states are found can be changed adiabatically, which leads to a change in the number of ingap states. The energy of the edge mode at  $v \rightarrow \infty$  will follow the dispersion of the

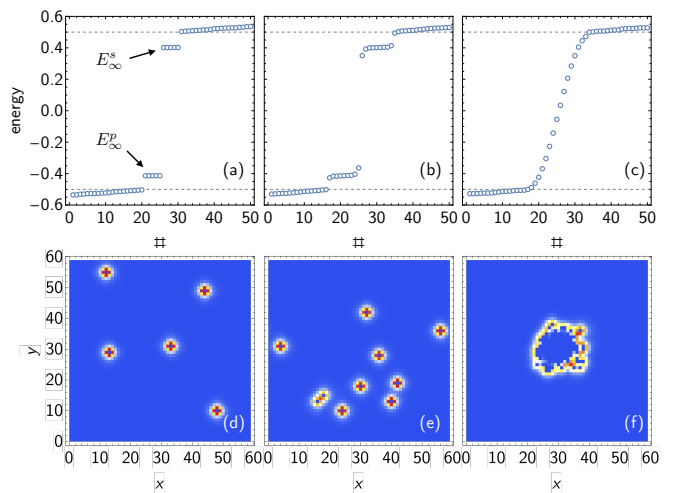


Figure 5. Ingap spectrum (a-c) and local ingap density of states (d-f) of random vacancies in a Chern insulator, defined in (18) with  $m = -0.5$ . The band edge is marked by a dashed gray line. (a,d) Dilute vacancies with minimal overlap between them, their energy is located at  $E_\infty^\sigma$  determined by the zeroes of  $\mu^\sigma$ . At each impurity site there are two ring states  $|\rho^s\rangle$  and  $|\rho^p\rangle$  located at the energy that minimizes the level repulsion of bands below and above the gap. Since in our model the lowest band is predominantly  $s$ , the  $p$  state is found at an energy  $E_\infty^p$  closest to the top of the valence band. (b,e) Increasing the density of impurities, some start overlapping, leading to delocalization around the small vacancy cluster and splitting in energy, deviating from  $E_\infty^\sigma$ . (c,f) Choosing the vacancies to be Gaussian distributed around the center of the sample, leads to a large vacant cluster. The ring states delocalize along the edge of the cluster filling the topological gap and gaining a linear dispersion seen by the equal energy spacing between states around zero energy. These are the boundary modes of the Chern insulator.

zeros in  $\mathcal{G}$ . Here, we wish to highlight that ring states, due to their spatial extent, hybridize with each other to form clusters of dispersing delocalized modes surrounding macroscopically large defects. To show this point, we present in Fig.5 a numerical simulation of random vacancies in a Chern insulator with varying density. If the vacancies are far apart, as shown in panels (a) and (d), they bind ring states at their pinning energies  $E_\infty^\sigma$  determined by the zeros of the local Green's function. When ring states come close to each other, they hybridize and split in energy, panel (b) and (e); finally evolving into the dispersive chiral modes surrounding large trivial puddles in the system, simulated in our case by choosing random vacancies with a Gaussian distribution centered at a particular position in the sample, panel (c) and (f). Note that in the last case, the number of ingap states does not match the number of impurities, or rank of  $\mathcal{V}$ , implying that when impurity states hybridize, a subset of them can be reabsorbed into the band continuum and become fully extended. The ingap states become delocalized around the impurity and gain a dispersion, as it can be concluded from the equal energy spacing of the energy states that

cross the topological gap.

#### IV. DISCUSSION

In this work, we have revealed a connection between band topology and the emergence of protected ingap impurity states, which we call ring states. We find that a local impurity  $\mathcal{V}$  at a position  $\mathbf{q}_0$  transforming under a representation  $\sigma$  defines a target band representation or atomic limit in the space group of the clean system. When the bands below and above the band gap are topologically distinct from this atomic limit, we find that ring states are necessary. The energies at which ring states are pinned to in the strong impurity limit reflect the zeros of the real part of the impurity projected Green's function,  $\mu(\omega) = \text{re} \langle \sigma, \mathbf{q}_0 | \mathcal{G}(\omega) | \sigma, \mathbf{q}_0 \rangle$  for  $|\sigma, \mathbf{q}_0\rangle$  the eigenstate of the impurity. Ring states are characterized by wavefunctions which are asymptotically orthogonal to  $|\sigma, \mathbf{q}_0\rangle$  while transforming under the same symmetry, assured by spatially avoiding the impurity site. The existence of ring states is a testament to the complex interplay between local perturbations and the geometry of the band structure, revealing length scales imprinted in the wavefunctions of the unperturbed Hamiltonian, rather than the structure of the impurity by itself.

We used the example of a Chern insulator to contextualize the concept of ring states. In this case, a trivial puddle within a topological bulk inevitably harbors a gapless state along its periphery. We could naively expect all ingap states to merge into the bulk bands upon shrinking the puddle to a single site vacancy due to the quantization of the edge spectrum. We have shown that, in fact, an ingap ring state necessarily persists all the way to the puddle being a single lattice site. Extending our analysis to other Wannier obstructed phases, we find that these are reflected in zeros of  $\mu^\sigma$ , which results in the formation of ring states, regardless of the presence or absence of gapless boundaries. These findings highlight the universality of ring states in topological materials and, therefore,

can serve as the elemental pieces for the construction of topological boundary states across the various topological phases. Exploring the ring state hybridization into various boundary states in distinct topological classes will be the focus of future research.

#### V. ACKNOWLEDGEMENTS

R.Q. acknowledges fruitful discussions with Haim Beidenkopf, Jed Pixley, Frank Schindler and Jennifer Cano. R.Q. and A.S. thank the Yukawa Institute for Theoretical Physics for hospitality. R.Q. is supported by the National Science Foundation under Award No. DMR-2340394 and Simons Foundation awards 990414 and 825870. R.I. is supported by the Israeli Science Foundation under grant No. 1790/18 and U.S.-Israel Binational Science Foundation (BSF) Grant No. 2018226. B.A.B. is supported by the European Research Council (ERC) under the European Union's Horizon 2020 research and innovation program (grant agreement No. 101020833), the ONR Grant No. N00014-20-1-2303, the Schmidt Fund for Innovative Research, Simons Investigator Grant No. 404513, the Gordon and Betty Moore Foundation through the EPiQS Initiative, Grant GBMF11070 and Grant No. GBMF8685 towards the Princeton theory program. Further support was provided by the NSF-MRSEC Grant No. DMR-2011750, BSF Israel US foundation Grant No. 2018226, the Princeton Global Network Funds. Z.-D. S. were supported by National Natural Science Foundation of China (General Program No. 12274005), Innovation Program for Quantum Science and Technology (No. 2021ZD0302403), National Key Research and Development Program of China (No. 2021YFA1401900). A.S. was supported by grants from the ERC under the European Union's Horizon 2020 research and innovation programme (Grant Agreements LEGOTOP No. 788715), the DFG (CRC/Transregio 183, EI 519/71), and the ISF Quantum Science and Technology (2074/19). The Flatiron institute is a division of the Simons Foundation.

- 
- [1] B. Bradlyn, L. Elcoro, J. Cano, M. Vergniory, Z. Wang, C. Felser, M. Aroyo, and B. A. Bernevig, Topological quantum chemistry, *Nature* **547**, 298 (2017), 1703.02050.
  - [2] C. Brouder, G. Panati, M. Calandra, C. Mourougane, and N. Marzari, Exponential Localization of Wannier Functions in Insulators, *Physical Review Letters* **98**, 046402 (2007), cond-mat/0606726.
  - [3] A. A. Soluyanov and D. Vanderbilt, Wannier representation of Z2 topological insulators, *Physical Review B* **83**, 035108 (2011), 1009.1415.
  - [4] R. Yu, X. L. Qi, A. Bernevig, Z. Fang, and X. Dai, Equivalent expression of Z2 topological invariant for band insulators using the non-Abelian Berry connection, *Physical Review B* **84**, 075119 (2011), 1101.2011.
  - [5] N. Read, Compactly supported Wannier functions and algebraic K-theory, *Physical Review B* **95**, 115309 (2017), 1608.04696.
  - [6] N. Marzari, A. A. Mostofi, J. R. Yates, I. Souza, and D. Vanderbilt, Maximally localized Wannier functions: Theory and applications, *Reviews of Modern Physics* **84**, 1419 (2012), 1112.5411.
  - [7] H. C. Po, H. Watanabe, and A. Vishwanath, Fragile Topology and Wannier Obstructions, *Physical Review Letters* **121**, 126402 (2018), 1709.06551.
  - [8] C. L. Kane and E. J. Mele, Quantum Spin Hall Effect in Graphene, *Physical Review Letters* **95**, 226801 (2005), cond-mat/0411737.
  - [9] D. Hsieh, D. Qian, L. Wray, Y. Xia, Y. S. Hor, R. J. Cava, and M. Z. Hasan, A topological Dirac insulator

- in a quantum spin Hall phase, *Nature* **452**, 970 (2008), 0902.1356.
- [10] H. Zhang, C.-X. Liu, X.-L. Qi, X. Dai, Z. Fang, and S.-C. Zhang, Topological insulators in Bi<sub>2</sub>Se<sub>3</sub>, Bi<sub>2</sub>Te<sub>3</sub> and Sb<sub>2</sub>Te<sub>3</sub> with a single Dirac cone on the surface, *Nature Physics* **5**, 438 (2009).
- [11] P. Roushan, J. Seo, C. V. Parker, Y. S. Hor, D. Hsieh, D. Qian, A. Richardella, M. Z. Hasan, R. J. Cava, and A. Yazdani, Topological surface states protected from backscattering by chiral spin texture, *Nature* **460**, 1106 (2009), 0908.1247.
- [12] M. Z. Hasan and C. L. Kane, Colloquium: Topological insulators, *Reviews of Modern Physics* **82**, 3045 (2010), 1002.3895.
- [13] M. Koenig, S. Wiedmann, C. Bruene, A. Roth, H. Buhmann, L. W. Molenkamp, X.-L. Qi, and S.-C. Zhang, Quantum Spin Hall Insulator State in HgTe Quantum Wells, *Science* **318**, 766 (2007), 0710.0582.
- [14] Q. Ma, A. G. Grushin, and K. S. Burch, Topology and geometry under the nonlinear electromagnetic spotlight, *Nature Materials* **20**, 1601 (2021), 2103.03269.
- [15] B. A. Bernevig, C. Felser, and H. Beidenkopf, Progress and prospects in magnetic topological materials, *Nature* **603**, 41 (2022), 2203.02890.
- [16] W. Kohn, Shallow Impurity States in Silicon and Germanium, *Solid State Physics* **5**, 257 (1957).
- [17] J. Bernholc and S. T. Pantelides, Scattering-theoretic method for defects in semiconductors. I. Tight-binding description of vacancies in Si, Ge, and GaAs, *Physical Review B* **18**, 1780 (1978).
- [18] G. A. Baraff and M. Schlüter, Self-Consistent Green's-Function Calculation of the Ideal Si Vacancy, *Physical Review Letters* **41**, 892 (1978).
- [19] H. P. Hjalmarson, P. Vogl, D. J. Wolford, and J. D. Dow, Theory of Substitutional Deep Traps in Covalent Semiconductors, *Physical Review Letters* **44**, 810 (1979).
- [20] M. Lannoo and J. Bourgoin, Point Defects in Semiconductors I, Theoretical Aspects, Springer Series in Solid-State Sciences , 68 (1981).
- [21] R. D. King-Smith, D. Vanderbilt, King-Smith, D. Vanderbilt, K.-S. RD, and R. D. King-Smith, Theory of polarization of crystalline solids, *Physical Review B* **47**, 1651 (1993), 1011.1669.
- [22] W. A. Benalcazar, B. A. Bernevig, and T. L. Hughes, Quantized electric multipole insulators, *Science* **357**, 61 (2017), arXiv: 1611.07987, 1611.07987.
- [23] I. Komissarov, T. Holder, and R. Queiroz, The quantum geometric origin of capacitance in insulators, arXiv 10.48550/arxiv.2306.08035 (2023), 2306.08035.
- [24] P. Y. Yu and M. Cardona, Fundamentals of Semiconductors, Physics and Materials Properties, Graduate Texts in Physics 10.1007/978-3-642-00710-1 (2010).
- [25] R.-J. Slager, L. Rademaker, J. Zaanen, and L. Balents, Impurity-bound states and Green's function zeros as local signatures of topology, *Physical Review B* **92**, 085126 (2015), 1504.04881.
- [26] Z. Ren, A. A. Taskin, S. Sasaki, K. Segawa, and Y. Ando, Large bulk resistivity and surface quantum oscillations in the topological insulator Bi<sub>2</sub>Te<sub>2</sub>Se, *Physical Review B* **82**, 241306 (2010), 1011.2846.
- [27] B. E. Feldman, M. T. Randeria, A. Gyenis, F. Wu, H. Ji, R. J. Cava, A. H. MacDonald, and A. Yazdani, Observation of a nematic quantum Hall liquid on the surface of bismuth, *Science* **354**, 316 (2016), 1610.07613.
- [28] M. T. Randeria, B. E. Feldman, F. Wu, H. Ding, A. Gyenis, H. Ji, R. J. Cava, A. H. MacDonald, and A. Yazdani, Ferroelectric quantum Hall phase revealed by visualizing Landau level wavefunction interference, *Nature Physics* **14**, 796 (2018), 1805.04533.
- [29] P. M. Tam, T. Liu, I. Sodemann, and L. Fu, Local probes for quantum Hall ferroelectrics and nematics, *Physical Review B* **101**, 241103 (2020), 2003.07851.
- [30] V. M. Pereira, F. Guinea, J. M. B. L. d. Santos, N. M. R. Peres, and A. H. C. Neto, Disorder Induced Localized States in Graphene, *Physical Review Letters* **96**, 036801 (2006), cond-mat/0508530.
- [31] T. Wehling, A. Black-Schaffer, and A. Balatsky, Dirac materials, *Advances in Physics* **63**, 1 (2014), 1405.5774.
- [32] M. M. Ugeda, I. Brihuega, F. Guinea, and J. M. Gómez-Rodríguez, Missing Atom as a Source of Carbon Magnetism, *Physical Review Letters* **104**, 096804 (2010), 1001.3081.
- [33] Z. Huang, D. P. Arovas, and A. V. Balatsky, Impurity scattering in Weyl Semimetals and their stability classification, *New Journal of Physics* **15**, 123019 (2013), 1310.0137.
- [34] P. K. Nag, N. Morali, R. Batyabal, A. Mazhar, M. Geier, P. Brouwer, C. Felser, B. Yan, N. Avraham, R. Queiroz, and H. Beidenkopf, From Ring States to Fermi Arc Modes in a Ferromagnetic Weyl Semimetal, unpublished.
- [35] M. Amani, D.-H. Lien, D. Kiriya, J. Xiao, A. Azcatl, J. Noh, S. R. Madhupathy, R. Addou, S. KC, M. Dubey, K. Cho, R. M. Wallace, S.-C. Lee, J.-H. He, J. W. A. III, X. Zhang, E. Yablonovitch, and A. Javey, Near-unity photoluminescence quantum yield in MoS<sub>2</sub>, *Science* **350**, 1065 (2015).
- [36] J. Xie, H. Zhang, S. Li, R. Wang, X. Sun, M. Zhou, J. Zhou, X. W. D. Lou, and Y. Xie, Defect-Rich MoS<sub>2</sub> Ultrathin Nanosheets with Additional Active Edge Sites for Enhanced Electrocatalytic Hydrogen Evolution, *Advanced Materials* **25**, 5807 (2013).
- [37] H.-P. Komsa and A. V. Krasheninnikov, Native defects in bulk and monolayer MoS<sub>2</sub> from first principles, *Physical Review B* **91**, 125304 (2015).
- [38] D. V. Lang, Deep-level transient spectroscopy: A new method to characterize traps in semiconductors, *Journal of Applied Physics* **45**, 3023 (1974).
- [39] L. Elcoro, B. Bradlyn, Z. Wang, M. G. Vergniory, J. Cano, C. Felser, B. A. Bernevig, D. Orobengoa, G. d. I. Flor, and M. I. Aroyo, Double crystallographic groups and their representations on the Bilbao Crystallographic Server, arXiv **50**, 1457 (2017), 1706.09272.
- [40] M. Aroyo, A. Kirov, C. Capillas, J. Perez-Mato, and H. Wondratschek, Bilbao Crystallographic Server. II. Representations of crystallographic point groups and space groups, *Acta Crystallographica Section A: Foundations of Crystallography* **62**, 115 (2006).
- [41] J. Zak, Symmetry Specification of Bands in Solids, *Physical Review Letters* **45**, 1025 (1980).
- [42] J. Zak, Band representations and symmetry types of bands in solids, *Physical Review B* **23**, 2824 (1981).
- [43] T. Thonhauser and D. Vanderbilt, Insulator/Chern-insulator transition in the Haldane model, *Physical Review B* **74**, 235111 (2006), arXiv:cond-mat/0608527, cond-mat/0608527.
- [44] A. A. Soluyanov and D. Vanderbilt, Smooth gauge for topological insulators, *Physical Review B* **85**, 115415 (2012), 1201.5356.

- [45] G. F. Koster and J. C. Slater, Wave Functions for Impurity Levels, *Physical Review* **95**, 1167 (1954).
- [46] J. Callaway, t Matrix and Phase Shifts in Solid-State Scattering Theory, *Physical Review* **154**, 515 (1967).
- [47] T. Tao, Topics in Random Matrix Theory, Graduate Studies in Mathematics 10.1090/gsm/132 (2012).
- [48] J. Cano, B. Bradlyn, Z. Wang, L. Elcoro, M. G. Vergniory, C. Felser, M. M. I. Aroyo, and B. A. Bernevig, Building blocks of topological quantum chemistry: Elementary band representations, *Physical Review B* **97**, 035139 (2018), 1709.01935.
- [49] This scenario can be avoided in one spatial dimension, where the band edge density of states diverges logarithmically.
- [50] B. A. Bernevig and S.-C. Zhang, Quantum Spin Hall Effect, *Physical Review Letters* **96**, 106802 (2006), cond-mat/0504147.
- [51] B. Bradlyn, Z. Wang, J. Cano, and B. A. Bernevig, Disconnected elementary band representations, fragile topology, and Wilson loops as topological indices: An example on the triangular lattice, *Physical Review B* **99**, 045140 (2019), 1807.09729.
- [52] E. N. Economou, *Green's functions in quantum physics*, Vol. 7 (Springer Science & Business Media).
- [53] A. C. Hewson, *The Kondo Problem to Heavy Fermions* (1993) pp. 411–418.
- [54] R. A. Horn and C. R. Johnson, *Matrix Analysis* (1985).
- [55] J. Cano, B. Bradlyn, Z. Wang, L. Elcoro, M. G. Vergniory, C. Felser, M. I. Aroyo, and B. A. Bernevig, Topology of Disconnected Elementary Band Representations, *Physical Review Letters* **120**, 266401 (2018), 1711.11045.
- [56] E. H. Lieb, Two theorems on the Hubbard model, *Physical Review Letters* **62**, 1201 (1989).
- [57] B. C. Carlson and J. M. Keller, Orthogonalization Procedures and the Localization of Wannier Functions, *Physical Review* **105**, 102 (1957).

# Supplementary information for “Ring states”

Raquel Queiroz, Roni Ilan, Zhida Song, B. Andrei Bernevig, and Ady Stern

## CONTENTS

I. Ring States	2
A. Topological obstructions	2
B. Impurity bound state from the Green’s function	3
C. Exact bound state solution for two flat bands	3
D. Level repulsion interpretation	5
E. Necessity of ring states in topological gaps	5
F. Ring states in dispersive bands	6
G. Spectral evolution of ring states	7
II. Ring state of a Chern insulator	8
III. Beyond rank 1 perturbations	9
IV. Discussion	10
V. Acknowledgements	10
References	10
A. Bound state from the Green’s function	13
B. Ring state wavefunctions in the flat band limit	16
C. Number of impurity states	18
D. Level repulsion	19
1. Discrete levels	19
2. Thermodynamic limit	20
E. Examples of $\mu^\sigma(\omega)$ in topological band insulators	21
1. Chern insulator from a band inversion	22
2. Topological insulator from a split band representation	22
F. Wannier obstruction and orbital projected states	26
G. Topological stability of ingap ring states	27
1. Necessity of zeros in $\mu(\omega)$ in a topological gap	27
2. Stability of zeros in $\mu^\sigma(\omega)$ in dispersive bands	28
3. Topologically enforced adiabatic discontinuity between unperturbed and perturbed bands	29
H. Exact solutions for ring state wavefunctions in the two-dimensional Chern insulator	30

### Appendix A: Bound state from the Green’s function

In this appendix, we review the form of bound states from a Green’s function perspective, which can be found in Refs. [52, 53]. Let us take the perturbed Hamiltonian,

$$\tilde{\mathcal{H}} = \mathcal{H} + \mathcal{V}, \tag{A1}$$

with  $\mathcal{V}$  a general perturbation of rank smaller than  $\mathcal{H}$ , and with both operators defined in the same Hilbert space. We can define the unperturbed resolvent Green’s function as

$$\mathcal{G}(\omega) = (\omega - \mathcal{H})^{-1}, \tag{A2}$$

and equivalently, the perturbed Green's function

$$\tilde{\mathcal{G}}(\omega) = (\omega - \tilde{\mathcal{H}})^{-1}, \quad (\text{A3})$$

which, when expressed in terms of the unperturbed Green's function, becomes

$$\tilde{\mathcal{G}}(\omega) = [1 - \mathcal{G}(\omega)\mathcal{V}]^{-1}\mathcal{G}(\omega). \quad (\text{A4})$$

Expanding the prefactor in a power series, we obtain the Dyson expansion

$$\tilde{\mathcal{G}}(\omega) = \mathcal{G}(\omega) + \mathcal{G}(\omega)\mathcal{V}\tilde{\mathcal{G}}(\omega) = \mathcal{G}(\omega) + \mathcal{G}(\omega)\mathcal{V}\mathcal{G}(\omega) + \mathcal{G}(\omega)\mathcal{V}\mathcal{G}(\omega)\mathcal{V}\mathcal{G}(\omega) + \dots \equiv \mathcal{G}(\omega) + \mathcal{G}(\omega)\mathcal{T}(\omega)\mathcal{G}(\omega), \quad (\text{A5})$$

where the T-matrix is defined. It can be rewritten in the convenient form

$$\mathcal{T}(\omega) = \mathcal{V}[1 - \mathcal{G}(\omega)\mathcal{V}]^{-1}. \quad (\text{A6})$$

The spectrum of the perturbed Hamiltonian corresponds to poles in the perturbed Green's function, which can occur perturbatively close to the poles of  $\mathcal{G}(\omega)$  in the band continuum, or, alternatively, as poles originating from the infinite sum in (A5) which appear in  $\mathcal{T}(\omega)$ . Considering the latter case, we look at eigenstates of  $\tilde{\mathcal{H}}$

$$(E - \mathcal{H})|\varphi_E\rangle = \mathcal{V}|\varphi_E\rangle \quad (\text{A7})$$

acting with  $\mathcal{G}(\omega)$  on both sides, we find the eigenstates must satisfy

$$|\varphi_E\rangle = \mathcal{G}(E)\mathcal{V}|\varphi_E\rangle \quad \text{or} \quad [1 - \mathcal{G}(E)\mathcal{V}]|\varphi_E\rangle = 0. \quad (\text{A8})$$

for  $E$  explicitly corresponding to the poles of  $\mathcal{T}(\omega)$  in (A6). For energies  $E$  outside the band continuum, the states  $|\varphi_E\rangle$  are bound states, while inside the band continuum, the states  $|\varphi_E\rangle$  are scattering states with a large overlap with the unperturbed states from the band. Namely, in the band continuum the solutions  $|\varphi_E\rangle$  satisfy the Lippman-Schwinger equation

$$|\varphi_E\rangle = |\psi_E\rangle + \mathcal{G}(E - i0^+)\mathcal{V}|\varphi_E\rangle \quad (\text{A9})$$

with  $|\psi_E\rangle$  the unperturbed eigenstates of  $\mathcal{H}$ .

Note that we consider impurities that do not bring new quantum degrees of freedom into the Hilbert space, but rather impart a local change in the potential affecting the states in the original Hilbert space. Therefore, the bound states created by the impurity will be reflected in the total density of states of the band, which will amount to a reduced number of states in the bands in favor of states outside the band. The change in the density of states at frequency  $\omega$  can be obtained from the imaginary part of the retarded Green's function,

$$\delta\nu(\omega) \equiv \tilde{\nu}(\omega) - \nu(\omega) = -\frac{1}{\pi} \text{im tr}[\tilde{\mathcal{G}}(\omega - i0^+) - \mathcal{G}(\omega - i0^+)], \quad (\text{A10})$$

where the trace is taken over the entire Hilbert space. Using the convenient relation

$$\text{tr} \mathcal{G}(\omega) = -\partial_\omega \log \det \mathcal{G}(\omega), \quad (\text{A11})$$

we find that

$$\delta\nu(\omega) = \frac{1}{\pi} \text{im} \partial_\omega \log \det [1 - \mathcal{G}(\omega - i0^+)\mathcal{V}]^{-1}, \quad (\text{A12})$$

and using the definition of the phase shift

$$\eta(\omega) = \arg \det \mathcal{T}(\omega - i0^+), \quad (\text{A13})$$

the change in density of states gets the simple form

$$\delta\nu(\omega) = \frac{1}{\pi} \partial_\omega \eta(\omega). \quad (\text{A14})$$

Note that to conserve the total number of states, the integrated density of states removed from a band must correspond to the number of bound states outside the band continuum. Therefore, the number of impurity-bound states is given by

$$N = - \int_{\text{bands}} \delta\nu(\omega) d\omega. \quad (\text{A15})$$

which is the sum of states that have been removed (by the addition of impurity) from the individual bands  $n_\alpha$ ,

$$N^\alpha = - \int_{\varepsilon_\alpha^{\min}}^{\varepsilon_\alpha^{\max}} \delta\nu(\omega) d\omega = \frac{1}{\pi} [\eta(\varepsilon_\alpha^{\max}) - \eta(\varepsilon_\alpha^{\min})] \quad (\text{A16})$$

where we consider that the bands are well separated in energy by energy gaps and delimited by the band-edge energies  $\varepsilon_\alpha^{\min}$  and  $\varepsilon_\alpha^{\max}$ .

Now let us consider an impurity of a specific form, with a single local eigenstate  $|\phi_0^\sigma\rangle$ . The perturbation is explicitly given by

$$\mathcal{V} = v |\phi_0^\sigma\rangle \langle \phi_0^\sigma|, \quad (\text{A17})$$

which amounts to adding a local energy to the orbital of symmetry character  $\sigma$  in the position  $\mathbf{q}_0$ . Choosing a basis that contains the state  $|\sigma\rangle$  the  $T$ -matrix has a single nonzero element given by

$$t^\sigma(\omega) = \langle \phi_0^\sigma | \mathcal{T}(\omega) | \phi_0^\sigma \rangle = v + v \langle \phi_0^\sigma | \mathcal{G}(\omega) | \phi_0^\sigma \rangle v + \dots = \frac{v}{1 - g^\sigma(\omega)v} \quad (\text{A18})$$

where

$$g^\sigma(\omega) \equiv \langle \phi_0^\sigma | \mathcal{G}(\omega) | \phi_0^\sigma \rangle \quad (\text{A19})$$

is the impurity projected Green's function. It follows that the  $T$ -matrix will only have poles at the solutions of  $g^\sigma(\omega) = 1/v$ . In particular, in the strong impurity limit  $v \rightarrow \pm\infty$ , its poles correspond to  $g^\sigma(\omega) = 0$ . These solutions can be captured by computing the real and imaginary parts of the retarded impurity projected Green's function

$$g^\sigma(\omega - i0^+) = \mu^\sigma(\omega) - i\pi\nu^\sigma(\omega). \quad (\text{A20})$$

with  $\nu^\sigma(\omega)$  the orbital-projected density of states. The density of states vanishes outside the band continuum, and therefore the bound state solutions are determined by the zeros of  $\mu^\sigma(\omega)$ . For  $v \rightarrow \pm\infty$ , we can expand  $t^\sigma$  as  $t^\sigma \sim -1/g^\sigma(1 + 1/g^\sigma v)$ , and therefore, we see the phase shift is determined by the phase of  $g^\sigma$ . We can write

$$\delta\nu^\sigma(\omega) \sim -\frac{1}{\pi} \partial_\omega \arg g^\sigma(\omega - i0^+), \quad (\text{A21})$$

which can be understood as follows: In the gap, when  $\partial_\omega \mu^\sigma(\omega)|_{\omega=E} < 0$  for an energy  $E$  at which there is a pole of the  $t^\sigma(\omega)$ , there is a positive change in density of states, that is, an added state. In the band, the change of density of states is spread throughout the band. A positive  $\partial_\omega \mu^\sigma(\omega) > 0$  implies that charge density is removed throughout the band, mostly from energies at which the phase of  $g^\sigma(\omega)$  changes substantially, i.e., the zero of  $\mu(\omega)$  and the band edges, see Fig.6. An accumulated  $\pi$  phase shift across the band implies that a full state is removed from the band. Note that if  $\mu^\sigma(\omega)$  does not cross zero with a positive slope through the band, there cannot be a total  $\pi$  phase shift.

We should note, by making use of a Kramers Krönig relation

$$\mu^\sigma(\omega) = \frac{1}{\pi} P \int d\omega' \frac{\nu^\sigma(\omega')}{\omega' - \omega} \quad (\text{A22})$$

with  $P$  the Cauchy principal value, that the information about the zeros in  $\mu^\sigma(\omega)$  and consequently the information about the bound states created by a strong local potential  $\mathcal{V}$ , is completely contained in the orbital resolved density of states  $\nu_0^\sigma(\omega)$  across the energy axis. In the following appendices and the main text, the subscript “0” indicating the bare Green's function is dropped since we do not explicitly use the perturbed Green's function in our analysis.

For concreteness, let us look at the example of a trivial two-dimensional band, obtained by a tight binding model on a square lattice, described by the Hamiltonian

$$\mathcal{H} = \sum_{\langle ij \rangle} -t c_i^\dagger c_j, \quad (\text{A23})$$

where  $c_i^\dagger$  creates a particle in the state  $|\phi_i\rangle$  at the Bravais lattice vector  $\mathbf{R}_i$ . The sum is taken over the nearest neighbors. The local Green's function, projected into the single orbital located at  $\mathbf{R}_0 = 0$  can be obtained by diagonalizing the Hamiltonian in reciprocal space

$$\varepsilon_{\mathbf{k}} = -2t(\cos k_x + \cos k_y), \quad (\text{A24})$$

and the local projected Green's function obtained from  $g(\omega) = \langle \phi_0 | \mathcal{G}(\omega) | \phi_0 \rangle = \int d\mathbf{k} (\omega - \varepsilon_{\mathbf{k}})^{-1}$ , which is shown in Fig. 6. A local perturbation of the form  $\mathcal{V} = v c_0^\dagger c_0$ , leads to a bound state at an energy given by  $g(\omega) = 1/v$ . For small  $v$  it corresponds to a state at the band edge, see Fig.6(b), which is taken to large energies as  $v \rightarrow \infty$ , leaving the band with one less state. Note that the change in the band's density of states is distributed across all energies in the band. Most of the spectral weight is removed from the band edges and the van Hove singularity where  $\partial_\omega \arg g(\omega)$  is the largest. There is a total phase shift  $\eta(\omega)$  of  $\pi$  across the band, corresponding to one bound state following (A16).

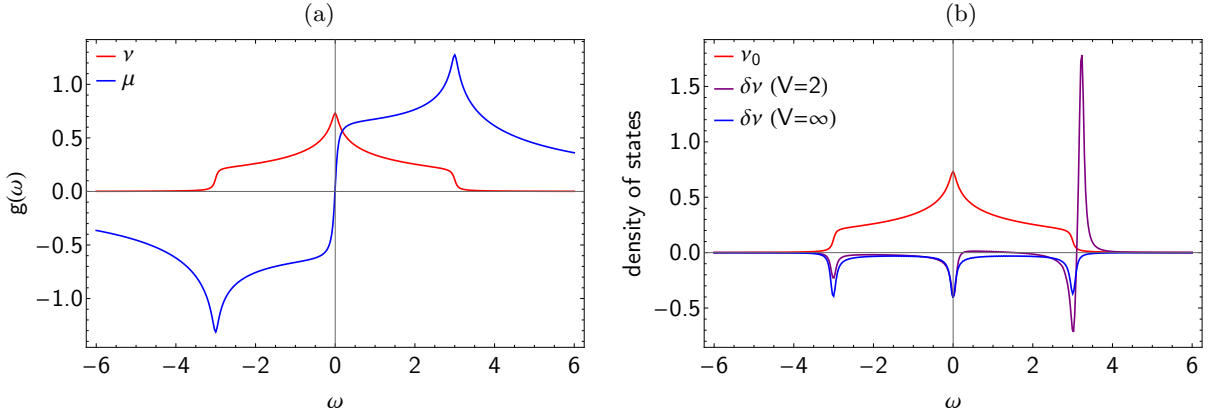


Figure 6. Local Green's function and density of states for a single atomic band, defined in (A23) with  $t = 1$ .

### Appendix B: Ring state wavefunctions in the flat band limit

In this appendix, we solve for the ring state energies and wavefunctions in the large  $v$  limit in a simple two-band flat Hamiltonian given by

$$\mathcal{H} = \sum_{\alpha=1,2} \varepsilon_{\alpha} \mathbb{P}^{\alpha} \quad (\text{B1})$$

with  $\mathbb{P}^{\alpha} = \sum_{\mathbf{k}} |\psi_{\mathbf{k}}^{\alpha}\rangle \langle \psi_{\mathbf{k}}^{\alpha}|$  the projector into the  $\alpha$  band, and  $\varepsilon_{\alpha}$  its energy, set without loss of generality to  $\varepsilon_1 = 0$  and  $\varepsilon_2 = \Delta$ , with  $\Delta$  the spectral gap. We consider that the Hamiltonian is perturbed by a rank-1 operator  $\mathcal{V}$  with a single eigenstate of energy  $v$ , given by

$$\mathcal{V} = v |\sigma\rangle \langle \sigma|. \quad (\text{B2})$$

As described in the main text, the perturbed Hamiltonian  $\mathcal{H} + \mathcal{V}$  contains bound states  $|\varphi_E\rangle$  at energy  $E$  that satisfy

$$|\varphi_E\rangle = \mathcal{G}(E) \mathcal{V} |\varphi_E\rangle = \sum_{\alpha} \frac{v \lambda_E}{E - \varepsilon_{\alpha}} |\Upsilon^{\alpha}\rangle, \quad \text{with } \lambda_E = \langle \sigma | \varphi_E \rangle \quad (\text{B3})$$

where  $|\Upsilon^{\alpha}\rangle \equiv \mathbb{P}^{\alpha} |\sigma\rangle$  are non-normalized band projections of the  $|\sigma\rangle$  state. They satisfy  $\langle \Upsilon^{\alpha} | \Upsilon^{\beta} \rangle = s_{\alpha} \delta_{\alpha\beta}$ , where  $s_{\alpha}$  is the integrated band overlap with the  $\sigma$  orbital over the band Bloch states, defined in the previous section. Therefore, the state  $|\sigma\rangle$  can be written as

$$|\sigma\rangle = \sum_{\alpha=1,2} \mathbb{P}^{\alpha} |\sigma\rangle = |\Upsilon^1\rangle + |\Upsilon^2\rangle. \quad (\text{B4})$$

From the normalization of  $|\sigma\rangle$  the projected norms satisfy  $s_1 + s_2 = 1$ . Let us rewrite  $s_1 = (1 - \delta s)/2$ ,  $s_2 = (1 + \delta s)/2$ . An obstructed band can be distinguished from a trivial band by the requirement that  $0 < s_{\alpha} < 1$  and consequently  $|\delta s| < 1$  for *any* choice of local state  $|\sigma\rangle$  in the Hilbert space of  $\mathcal{H}$  that preserves the local site symmetry.

In the large  $|v|$  limit, there are two possible solutions of Eq.(B3), with energies outside the spectral continuum which are qualitatively distinct. One solution has an energy of order  $O(v)$ . It corresponds to a solution approaching the eigenstate of  $\mathcal{V}$ ,  $\langle \sigma | \varphi_E \rangle \rightarrow 1$ . Let us call this solution  $|\sigma_E\rangle$  and write it as

$$|\sigma_E\rangle = (1 + a) |\Upsilon^1\rangle + (1 + b) |\Upsilon^2\rangle = |\sigma\rangle + O(1/v), \quad (\text{B5})$$

with  $a$  and  $b$  small parameters of order  $O(1/v)$ . The parameters  $a$  and  $b$  depend on the energy of the bound state as a function of  $v$ , as it will be derived below. The second state must be orthogonal to  $|\sigma_E\rangle$ . For that state  $\tilde{v}_E$  remains finite as  $v \rightarrow \infty$ , that is  $\langle \sigma | \varphi_E \rangle \rightarrow 0$ . The energy of the  $|\rho_E\rangle$  state remains of order  $O(1)$ , between the minimum and maximum eigenvalues of the unperturbed Hamiltonian  $\mathcal{H}$ . The finite energy state,  $|\rho_E\rangle$  is orthogonal to  $|\sigma_E\rangle$  by avoiding the impurity site  $\mathbf{q}_0$ . Orthogonality with  $|\sigma\rangle$  at  $v = \pm\infty$  fixes the asymptotic form of this state to be

$$|\rho\rangle = \sqrt{\frac{s_1}{s_2}} |\Upsilon^2\rangle - \sqrt{\frac{s_2}{s_1}} |\Upsilon^1\rangle, \quad (\text{B6})$$



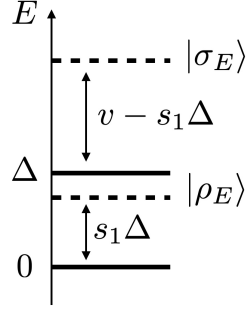


Figure 7. Energy spectrum of  $\mathcal{H} + \mathcal{V}$  in the large  $v$  limit for the model of two perfectly flat bands, up to order  $O(1/v)$  for  $v > 0$ .

satisfying  $\mathcal{V}|\rho\rangle = 0$ . Note that  $|\rho\rangle$  is not itself an eigenstate of  $\mathcal{H} + \mathcal{V}$ . The exact eigenstate of the perturbed Hamiltonian  $\mathcal{H} + \mathcal{V}$  at a finite energy  $E$ ,  $|\rho_E\rangle$  is close to  $|\rho\rangle$ , deviating by the same small parameters  $a$  and  $b$  of order  $O(1/v)$ ,

$$|\rho_E\rangle = (1+b)\frac{\sqrt{1-\delta s}}{\sqrt{1+\delta s}}|\Upsilon^1\rangle - (1+a)\frac{\sqrt{1+\delta s}}{\sqrt{1-\delta s}}|\Upsilon^2\rangle = |\rho\rangle + O(1/v), \quad (\text{B7})$$

The form presented above guarantees that both states are orthogonal and normalized as long as the

$$\frac{1}{2}(a+1)^2(1-\delta s) + \frac{1}{2}(b+1)^2(1+\delta s) = 1. \quad (\text{B8})$$

We now fix  $a$  and  $b$  by taking both  $|\sigma_E\rangle$  and  $|\rho_E\rangle$  states to be eigenstates of  $\mathcal{H} + \mathcal{V}$ . First, we can calculate their energies from the inner product of  $|\sigma\rangle$  and Eq.(B3), which gives a quadratic equation for the energy  $E$ ,

$$\frac{1}{v} = \frac{s_1}{E - \varepsilon_1} + \frac{s_2}{E - \varepsilon_2}, \quad (\text{B9})$$

with two solutions

$$E_{\pm} = \frac{1}{2}(\Delta + v \pm \sqrt{\Delta^2 + 2v\delta s\Delta + v^2}). \quad (\text{B10})$$

Assuming  $v\delta s > 0$ , we find

$$E_+ \sim v + \Delta(1 - \delta s)/2 = s_2\Delta + v = \Delta + v - s_1\Delta, \quad (\text{B11})$$

and

$$E_- \sim \Delta(1 + \delta s)/2 = s_1\Delta, \quad (\text{B12})$$

approximate to first order in  $1/v$ . The energies  $E_{\pm}$  deviate from the original band energies as long as  $|\delta s| \neq 1$ . Expanded to order  $O(1/v)$ , we can associate the largest energy with the  $|\sigma_E\rangle$  state, and the lowest energy to the ring state  $|\rho_E\rangle$ ,

$$E_{\pm} = \frac{1}{2}[v(1 \pm 1) + \Delta(1 \pm \delta s)] \pm (\delta s^2 - 1)\frac{\Delta}{4v} + O(1/v^2). \quad (\text{B13})$$

It is important to make two remarks here. First, in a topological phase, *both* energies  $E_{\pm}$  will correspond to bound states outside the original unperturbed bands. The ingap state  $|\rho_E\rangle$  is separated from the flat bands by an energy  $\Delta s_{\alpha}$ , of order  $O(1)$  and independent of  $v$ , for all possible choices of  $\mathcal{V}$ . In a trivial band, there is always a choice of  $\mathcal{V}$  such that the ring state solution does not exist. Second, the geometric overlap with the band states determines the finite energy separation of the ring state from the band edge. As we see below, it can be understood as the result of the level repulsion between the ring states and the band eigenstates. The energy of the ring state depends only on the energy gap and the overlap  $s_{\alpha}$ , becoming independent of  $v$  for large enough strength  $v \gg \Delta$ .

Using the expressions for  $E_{\pm}$ , we take

$$\langle \sigma_E | (\mathcal{H} + \mathcal{V}) | \sigma_E \rangle = E_+, \quad \langle \rho_E | (\mathcal{H} + \mathcal{V}) | \rho_E \rangle = E_-, \quad (\text{B14})$$

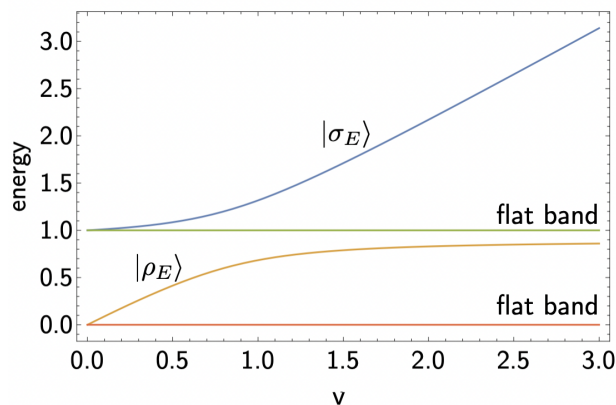


Figure 8. Evolution of the bound state energies in the flat band model for  $\Delta = 1$ ,  $\delta s = 0.9$ .

to find the solutions for the small parameters  $a$  and  $b$ ,

$$a = -\frac{\Delta}{v}(1 + \delta s) + O(1/v^2), \quad b = \frac{\Delta}{v}(1 - \delta s) + O(1/v^2) \quad (\text{B15})$$

which are both non-vanishing provided  $|\delta s| > 0$  as it is necessarily the case for topological bands.

As a sanity check, we look at the topologically trivial flat band case with  $\delta s = 1$ ,  $s_1 = 0$ ,  $s_2 = 1$ , and  $v > 0$ . In this case,  $E_+ = v + \varepsilon_2 = v + \Delta$  and  $E_- = \varepsilon_1 = 0$ . Since only the  $\alpha = 2$  has nonzero matrix elements with  $\mathcal{V}$ , the orbital  $|\sigma\rangle$  is removed from this band without obstruction or creating a ring state. Here,  $a = -\Delta/v$  while  $b = 0$  and the ring state solution does not exist. Both forms (B6) and (B7) are not well defined.

Finally, let us note that since any symmetry  $\hat{g}$  operator that commutes with the Hamiltonian  $\hat{g}\mathcal{H} = \mathcal{H}\hat{g}$  also commutes with the band projectors  $\hat{g}\mathbb{P}^\alpha = \mathbb{P}^\alpha\hat{g}$  it follows that both  $|\sigma_E\rangle$  and  $|\rho_E\rangle$  transform under the same symmetry representation. Their orthogonality comes from spatially avoiding each other.

### Appendix C: Number of impurity states

The number of bound states expected from a local perturbation  $\mathcal{H} + \mathcal{V}$ , is highly constrained by the spectrum of  $\mathcal{H}$  and  $\mathcal{V}$  separately. We use Weyl's inequalities [54], which state that the perturbed eigenvalues  $E_i$ , for  $i = 1, \dots, N$  organized in descending order (with  $N$  the total number of eigenstates) satisfy

$$\varepsilon_j + v_k \leq E_i \leq \varepsilon_r + v_s, \quad j + k - N \geq i \geq r + s - 1. \quad (\text{C1})$$

where  $\varepsilon_i, v_i$  are the eigenvalues of the unperturbed Hamiltonian and the perturbation, respectively. The unperturbed energies reach from  $\varepsilon_1 = \varepsilon_{\max}$  to  $\varepsilon_n = \varepsilon_{\min}$ . In the simple case where  $\mathcal{V}$  is a rank 1 operator with a single nonzero eigenvalue,  $v_1 = v$  and  $v_{k \neq 1} = 0$ , and  $v \gg \varepsilon_1$ , the above inequality tells us that there is a single energy above  $\varepsilon_1$ . Namely, taking  $i = 1$  we find

$$\varepsilon_1 \leq E_1 \leq \varepsilon_1 + v, \quad (\text{C2})$$

and

$$\varepsilon_2 \leq E_2 \leq \varepsilon_1. \quad (\text{C3})$$

which is the tightest bound on  $E_2$  given a large  $v$ . These inequalities imply that there can exist a single perturbed energy above the spectrum of  $\mathcal{H}$ . Analogously if  $v \ll \varepsilon_i$  there can only exist a single bound state below the unperturbed spectrum. In these limits, the previous inequalities amount to Cauchy's interlacing theorem [54], which effectively removes one column and one row from the perturbed Hamiltonian. In particular, the interlacing theorem tells us that the perturbed system has energy states  $E_i$  satisfying

$$\varepsilon_i \leq E_i \leq \varepsilon_{i-1}. \quad (\text{C4})$$

and therefore, within a gap, a rank 1 perturbation  $\mathcal{V}$  can create, at most, a single bound state. There can only exist more than one state in the gap if there are more nonvanishing eigenstates of  $\mathcal{V}$ , as it is in the case of a multi-orbital or multi-site vacancy.

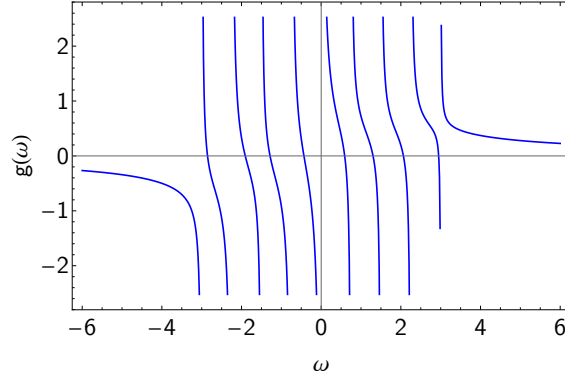


Figure 9. Poles of  $g(\omega)$  in a single orbital tight binding Hamiltonian A23 with periodic boundaries and a finite size of  $6 \times 6$ . The local Green's function diverges at every energy eigenvalue and decays monotonically otherwise [45]. There are 9 distinct poles, and a zero in between each pole corresponds to an attractive fixed point of the perturbed spectrum. Outside the band, there is one zero at  $\omega = \pm\infty$  which allows for the removal of a single state from the band by a local perturbation, whose energy  $E \rightarrow v$  as  $v \rightarrow \pm\infty$ .

## Appendix D: Level repulsion

### 1. Discrete levels

The exact energy at which the eigenvalues of a perturbed Hamiltonian  $E_i$  are found depends on the structure of their wavefunctions and can be obtained by the Hadamard variation formulas [47]. Let us interpret the strength of the perturbation  $\mathcal{V}$  as a time  $t$ , and let  $t \rightarrow \infty$  in the following way

$$\mathcal{H}(t) = \mathcal{H} + t\hat{\mathcal{V}} \quad (\text{D1})$$

where  $\hat{\mathcal{V}} = |\sigma\rangle\langle\sigma|$  is the normalized perturbation. The eigenvalues of the (finite dimension) Hamiltonian  $\mathcal{H}(t)$  are deformed adiabatically as a function of  $t$ , satisfying the differential equations

$$\dot{\epsilon}_n = \langle\psi_n|\hat{\mathcal{V}}|\psi_n\rangle = s_n, \quad (\text{D2})$$

known as the first Hadamard variation formula, and

$$\ddot{\epsilon}_n = 2 \sum_{m \neq n} \frac{|\langle\psi_m|\hat{\mathcal{V}}|\psi_n\rangle|^2}{\epsilon_m - \epsilon_n}, \quad (\text{D3})$$

known as the second Hadamard variation formula. The second formula can be interpreted as follows. The eigenstates at a time  $t$  feel a level repulsion from states close by in energy, provided the matrix elements of  $\hat{\mathcal{V}}$  that couple them to  $\epsilon_n$  do not vanish. The level repulsion is expressed as an effective force that acts on the eigenenergies  $\epsilon_n$ , with the opposite sign for states below or above  $\epsilon_n$ . It is particularly insightful to rewrite the previous expression with an explicit dependence on the resolvent Green's function

$$\mathcal{G}(\omega) = \sum_m \frac{|\psi_m\rangle\langle\psi_m|}{\omega - \epsilon_m} \quad (\text{D4})$$

which implies for  $\mathcal{V} = |\sigma\rangle\langle\sigma|$ , Eq.(D3) is given by

$$\ddot{\epsilon}_n = 2s_n \sum_{m \neq n} \frac{|\langle\sigma|\psi_m\rangle|^2}{\epsilon_m - \epsilon_n} \quad (\text{D5})$$

on the right-hand side the projected Green's function appears up to the pole of  $\epsilon_n$ , thus we write it as

$$\ddot{\epsilon}_n = 2s_n \mathcal{P}g^\sigma(\epsilon_n) \quad (\text{D6})$$

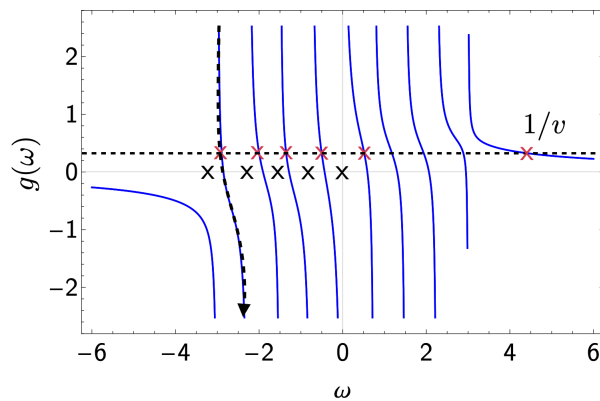


Figure 10. Evolution of the local spectrum of a single band given a local perturbation  $\mathcal{V} = v|\sigma\rangle\langle\sigma|$ . The unperturbed poles are marked with a black cross, and the perturbed solutions are marked in red. A single solution lays outside the band, which corresponds to the bound state, whose strong coupling fixed point is at  $v = \pm\infty$ . This is consistent with the fact that only one single eigenenergy of the perturbed system exceeds the unperturbed bandwidth, as discussed in App.C.

with  $s_n = |\langle\psi_n|\sigma\rangle|^2$  and  $g^\sigma(\omega) = \langle\sigma|\mathcal{G}(\omega)|\sigma\rangle$ . The operator  $\mathcal{P}$  is defined such that it removes the pole at  $\varepsilon_n$  from the projected Green's function. Therefore  $\mathcal{P}g^\sigma(\varepsilon_n)$  can be interpreted as the force exerted on the eigenstate  $\varepsilon_n$  from all other states in the system, once  $\mathcal{V}$  is turned on. Note that if  $s_n = 0$  the impurity does not couple with the  $|\psi_n\rangle$  eigenstate and therefore, its energy remains unchanged. Furthermore, the energy  $\varepsilon_n$  is not repelled from states that do not couple to the impurity.

In a finite size system, typical extended levels with  $\varepsilon_n$  within the band, experience an opposing force from the energy levels  $\varepsilon_m$  above and below  $\varepsilon_n$ , proportional to  $v^2 s_n (\varepsilon_m - \varepsilon_n)^{-1}$ , which vanishes at a finite energy in between the unperturbed poles since the total force diverges with opposite signs when approaching consecutive poles, see Fig.9. The level repulsion is of the order  $O(1/N)$ , as expected in a band continuum. This implies that given a local perturbation with a single eigenstate, all eigenstates are weakly perturbed to find a new energy that sits in between the original unperturbed energies. However, the states at band edges behave differently. At infinitesimal time  $t$ , a state at the band edge with a nonvanishing overlap  $s_n$  will be pushed out of the band since it does not experience a counteracting force. At  $t \rightarrow \infty$  this eigenstate energy will converge to an attractive fixed point of Eq.(D3), where both sides of the equation vanish outside the band continuum.

As the state  $\varepsilon_n$  is removed from the band continuum, it becomes localized around the impurity. One would expect the level repulsion from each delocalized state to be small. Therefore in a trivial multiband system, the localized state can cross high-energy bands and find its final energy at  $E = \pm\infty$ . However, as we have argued in the main text,  $g(\omega)$  can have finite energy zeroes within energy gaps. These fixed points, which we denote *ingap spectral attractors* indicate that the bands above and below the final energy of the localized state exert an equal force of this state such that it cannot be removed from the gap by varying  $v$ .

## 2. Thermodynamic limit

In the thermodynamic limit, the vast majority of states are weakly affected by  $\mathcal{V}$ , remaining extended through the entire sample. Therefore, we are only interested in the effect of  $\mathcal{V}$  on states outside the band continuum, which are bound at the impurity site. The collective effect of the band on the impurity bound level can be obtained by adding a small imaginary part to  $\mathcal{G}(\omega)$  such that the impurity projected Green's function,

$$g^\sigma(\omega - i0^+) = \mu^\sigma(\omega) - i\pi\nu^\sigma(\omega) \quad (\text{D7})$$

dictates the slow spectral migration of the impurity-bound states at energy  $E$ , which at  $t = 0$  corresponds to the state at the band extrema. Outside the band continuum, we get exactly

$$\ddot{E} = 2\lambda_E^2 \mu^\sigma(E), \quad (\text{D8})$$

since the real part of  $g^\sigma(\omega - i0^+)$  excludes the pole at  $\omega$  through Cauchy's principal part (the continuum limit of  $\mathcal{P}$  defined in the previous section). Here,  $\lambda_E = \langle\sigma|\psi_E\rangle$ , for  $|\psi_E\rangle$  the band-edge eigenstate of the unperturbed system.

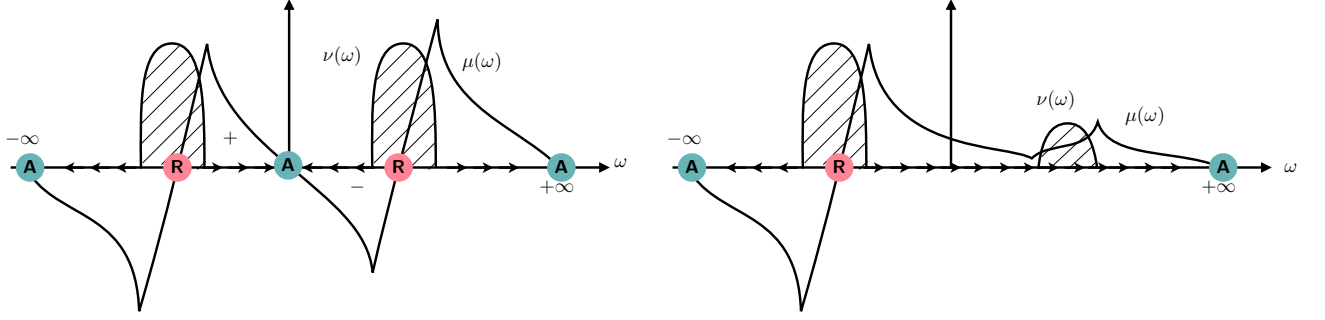


Figure 11. Scheme of the general form of the eigenstates of the impurity projected Green's function in dispersive bands. Zeros of  $\mu(\omega)$  correspond to spectral attractors (A) or repellers (R) according to their slope, fixed points of Eq.D3. The arrows indicate the flow of the bound state created by the impurity to the strong impurity limit. The existence of an ingap attractor is required for topological bands, independently of their dispersion; while it is absent or can be removed symmetrically and adiabatically in unobstructed bands.

Up to non-universal proportionality factors, the bound state energy satisfies

$$\ddot{E} \propto \mu^\sigma(E), \quad (\text{D9})$$

as stated in the main text. That is, the real part of the impurity projected Green's function  $\mu^\sigma(E)$  can be interpreted as a “force” that is exerted on a bound state at energy  $E$  given a perturbation  $\mathcal{V} = v |\sigma\rangle \langle\sigma|$ , weighted by how much the state couples to  $\mathcal{V}$ ,  $s_E$ . Therefore, a zero in  $\mu^\sigma(E)$  reflects a stable fixed point to which the bound state energy converges at large  $v$ . Note that from (D2)  $s_E$  can be interpreted as a velocity, which tells us how fast the state is removed from the band.

Again, also in the thermodynamic limit there is always a fixed point at  $E = \pm\infty$ , but important are instances in which zero occurs in the spectral gap of  $\mathcal{H}$ . These correspond to points at which the bands above and below the bound state repel it in equal strength. In these cases, the energy at which the bound state exists is a fixed point that depend only on the eigenstate of the impurity and only weakly its strength.

Let us return to the exactly solvable flat band limit of Sec.A. A zero in  $\mu^\sigma(\omega)$  exists provided both  $s_\alpha$  do not vanish. Let us rewrite the degenerate band energies in a symmetric way  $\varepsilon_1 = -\Delta/2$  and  $\varepsilon_2 = +\Delta/2$ , and  $\delta s = (s_1 - s_2)/2$ . The effective force on the state at energy  $E$  for an attractive potential is proportional to

$$\mu^\sigma(E) = \frac{s_1}{E + \Delta/2} + \frac{s_2}{E - \Delta/2} = \frac{E - \Delta\delta s}{E^2 - (\Delta/2)^2} \quad (\text{D10})$$

There is a spectral attractor at  $E = \Delta\delta s$  provided  $|\delta s| < 1$ , as it is the case of topological bands for every possible  $\sigma$ . A finite bandwidth of the topological bands will quantitatively change the effective force experienced by the ingap state and, consequently, change the energy of the fixed point.

### Appendix E: Examples of $\mu^\sigma(\omega)$ in topological band insulators

In this section, we look at the evolution of the real part of the local Green's function in distinct models and parameters. We have seen that  $\mu^\sigma(\omega)$  can be interpreted as the effective force experienced by the band eigenstates in the presence of a local perturbation of rank 1 with nonzero eigenstate  $|\sigma\rangle$ . Its zeros correspond to fixed points in the strong coupling limit to the local impurity. As a guiding principle, we choose the state  $\sigma$  that maximizes the overlap with the filled bands of energy below the chemical potential. The chemical potential is without loss of generality set to zero in all models.

For the trivial band presented in Fig.6, there is a single zero in the real part  $\mu(\omega) = \text{re } g(\omega - i0^+)$  in the middle of the band, corresponding to an unstable fixed point for the eigenvalues in the presence of a local scalar potential. That is, the band tends to spread its density of states above and below the band.

### 1. Chern insulator from a band inversion

Let us consider a two-band model on a square lattice, given by

$$\mathcal{H} = \sum_{ij} h_{ij}^{\sigma\tau} c_{i\sigma}^\dagger c_{j\tau} \quad (\text{E1})$$

with  $c_{i\sigma}^\dagger$  creating an electron in the orbital state  $|\phi_i^\sigma\rangle$  with  $i, j$  spatial indices and  $\sigma, \tau$  orbital indices labelling the eigenstates of  $\sigma_z$ ,  $\sigma_z |s\rangle = +|s\rangle$  and  $\sigma_z |p\rangle = -|p\rangle$ . In reciprocal space,

$$\mathcal{H} = \sum_{\mathbf{k}} c_{\mathbf{k}}^\dagger H(\mathbf{k}) c_{\mathbf{k}}, \quad (\text{E2})$$

with  $c_{\mathbf{k}}^\dagger = (c_{\mathbf{k},s}^\dagger, c_{\mathbf{k},p}^\dagger)$  and the momentum space Hamiltonian taking the simple two-band form

$$H(\mathbf{k}) = (m + 4b - 2b \cos k_x - 2b \cos k_y) \sigma_z - v \sin k_x \sigma_x - v \sin k_y \sigma_y \quad (\text{E3})$$

Taking  $b, v > 0$ , the model admits a Chern insulator phase for  $-8b < m < 0$ , where the Chern number changes sign at  $m = -2b$ . Around  $m = 0$ , the Hamiltonian can be expanded around  $k = 0$ , becoming

$$H(\mathbf{k}) = (m + bk^2) \sigma_z - v \mathbf{k} \cdot \boldsymbol{\sigma} + O(k^3) \quad (\text{E4})$$

which is the same model used in Eq.18 in the main text. At  $m < 0$ , the filled band has a majority of  $s$  character. A topological phase transition occurs by closing the spectral gap at  $k = 0$ , at which point the filled Bloch eigenstate at  $k = 0$  switches orbital character. This structure can be appreciated by looking at the  $s$ -orbital projected local Green's function, which can be seen in Fig.13. The real  $\mu^\sigma(\omega)$  for  $\sigma = s$  acquires a zero of negative slope in the band gap at the topological phase, corresponding to a spectral attractor at a finite energy, a scenario unique to multiband Hamiltonians. This can be seen explicitly in Fig.14 by the appearance of a negative region bounded by zeros of the opposite slope. In the equations of motion defined in the previous section, this zero corresponds to a stable fixed point at a finite energy at which the bound state converges to in the strongly coupled impurity limit.

In Fig.13 we take a closer look at the evolution of the density of states  $\nu^\sigma(\omega)$  and  $\mu^\sigma(\omega)$  across the band inversion, where the band edges with opposite orbital character are interchanged. Since we look at a two-dimensional model, the projected density of states is expected to diverge at the band edge associated with the  $\sigma$  band. At the topological phase transition, the top band edge of the  $s$  band is interchanged with the bottom band edge of the  $p$  band, leading to a shift in the divergence in  $\mu^\sigma(\omega)$  from the filled to the empty band. This process comes together with the creation of the ingap zero and the protected ring state in the presence of a strong impurity. In Fig.?? we show that the shape of the band edge does not affect the existence of a zero in  $\mu^\sigma(\omega)$ .

### 2. Topological insulator from a split band representation

Another example worth considering is the case of graphene, with a very small energy gap determined by spin-orbit coupling. In this case, the topological bands are not formed by a band inversion around high symmetry momenta, rather, their topology results from the partial filling of a split elementary band representation [55]. The model is given by Kane-Mele's model [8] written in terms of the nearest-neighbor and next-nearest neighbor hopping terms

$$\mathcal{H} = \mathcal{H}_0 + \mathcal{H}_R + \mathcal{H}_{KM} \quad (\text{E5})$$

with

$$\mathcal{H}_0 = -t \sum_{\langle ij \rangle} c_i^\dagger c_j \quad (\text{E6})$$

for  $c_i^\dagger = (c_{i\uparrow}^\dagger, c_{i\downarrow}^\dagger)$ . Note there are two sublattices, and a total of  $4N$  Bloch states. The Rashba Hamiltonian is given by

$$\mathcal{H}_R = \frac{\alpha}{2i} \sum_{\langle ij \rangle} c_i^\dagger (\boldsymbol{\sigma} \times \mathbf{d}_{ij}) c_j \quad (\text{E7})$$

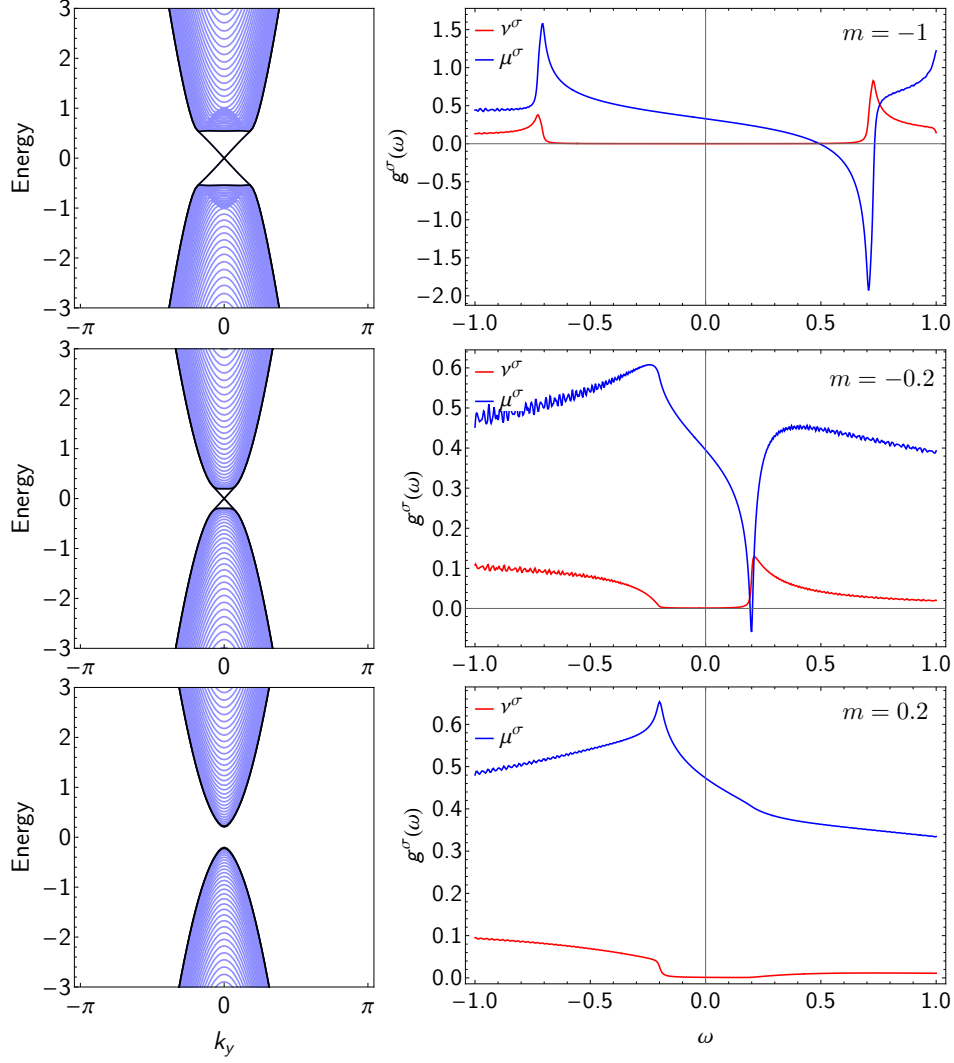


Figure 12. Energy spectrum of Hamiltonian (E3) with open boundaries and impurity projected Green's function, with impurity state defined by  $\sigma_z |\sigma\rangle = -|\sigma\rangle$ . In all three plots we choose  $v = 1$  and  $b = 3$ . Note that the shape of the band edge in the topological phase does not influence the existence of the zero in  $\mu^{\sigma}(\omega)$ , which is created in the gap closing transition.

for  $\mathbf{d}_{ij} = \mathbf{q}_i - \mathbf{q}_j$  and a staggered hopping that gaps the Dirac points at  $K$  and  $K'$  momenta

$$\mathcal{H}_{KM} = \frac{\beta}{2i} \sum_{\langle\langle ij \rangle\rangle} c_i^{\dagger} (\nu_{ij} \sigma_z) c_j \quad (\text{E8})$$

for  $\nu_{ij} = \pm 1$  alternating clockwise for the six next nearest neighbors to a given site.

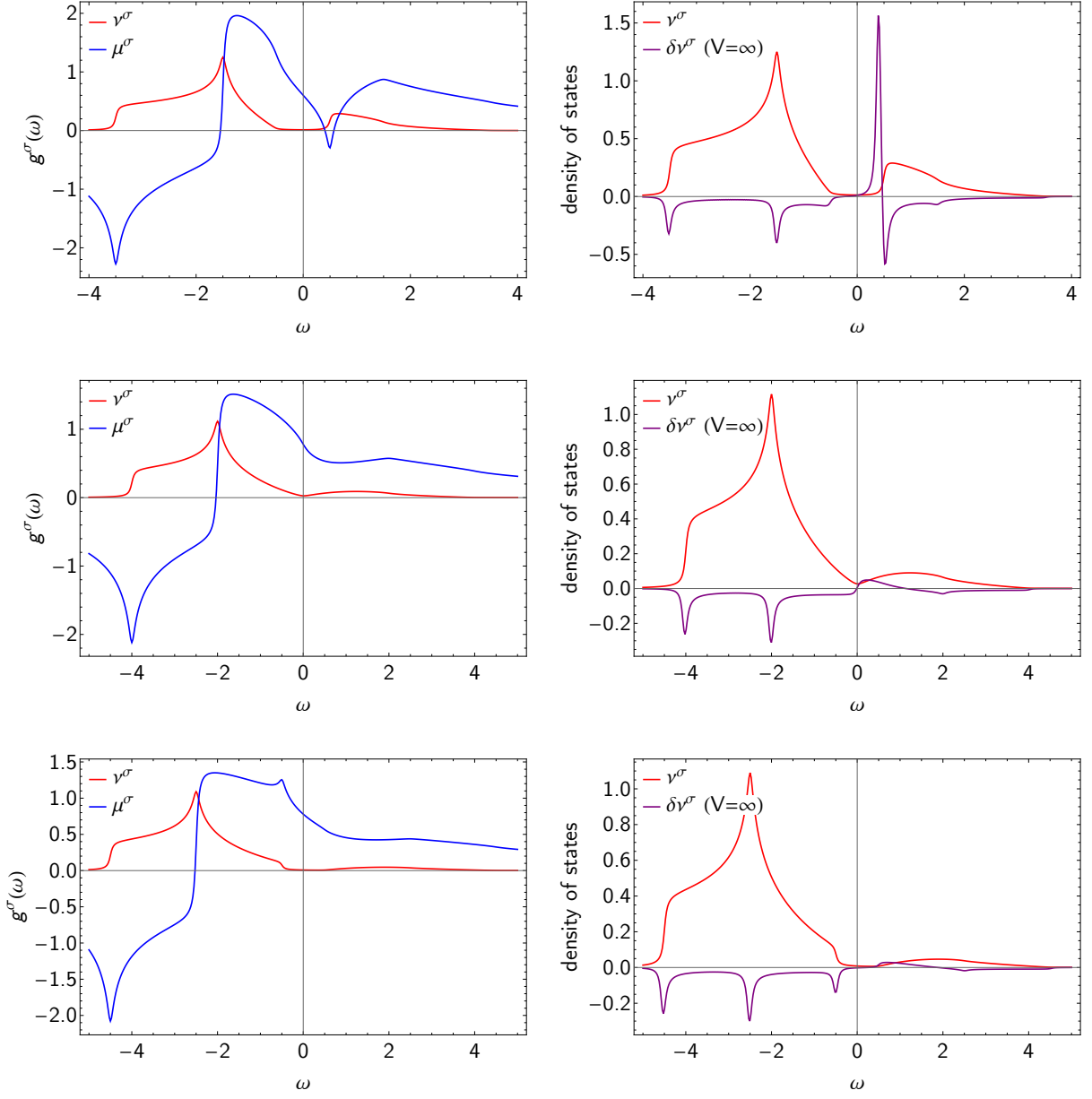


Figure 13. Left: Evolution of the local projected Green's function  $g^\sigma(\omega) = \mu^\sigma(\omega) - i\pi\nu^\sigma(\omega)$  as a function of the mass parameter  $m$  across a topological phase transition. Right: The density of states, and the change in the density of states in the strong impurity limit. Upper row:  $M = -0.5$ , topological phase; Middle row:  $M = 0$ , topological phase transition; lower row:  $M = +0.5$ , trivial phase. Across the topological phase transition, the zero of  $\mu^\sigma(\omega)$  is removed, and with it the ingap bound state at  $v \rightarrow \infty$ , present in the topological case as a sharp peak of positive change in density of states,  $\delta\nu^\sigma > 0$ . Only exactly at the topological phase transition  $\mu^\sigma(\omega)$  loses its divergence and is smooth across the Dirac point. Note that we assume that the ring state does not overlap trivially with a band which it shares no matrix elements with.



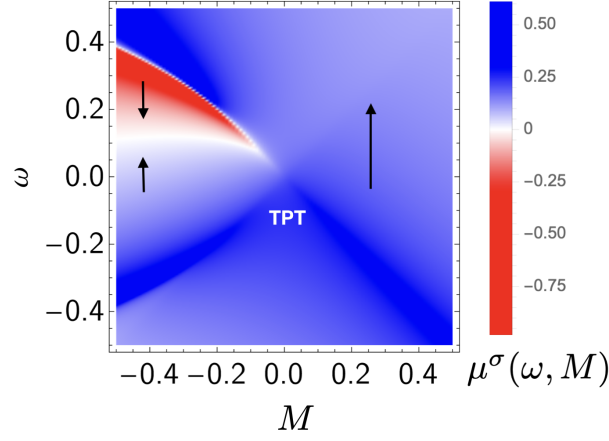


Figure 14. Phase diagram of  $\mu^\sigma(\omega)$  for  $\sigma = s$  in the (continuum) Chern insulator model for small mass. The topological phase transition (TPT) is characterized by the appearance of a zero of negative slope (attractor), and one of positive slope (repeller) together a region  $\mu^\sigma(\omega) < 0$ , which corresponds to an effective negative force on ingap bound states that traps the ring state in the gap, due to the ingap stable fixed point.

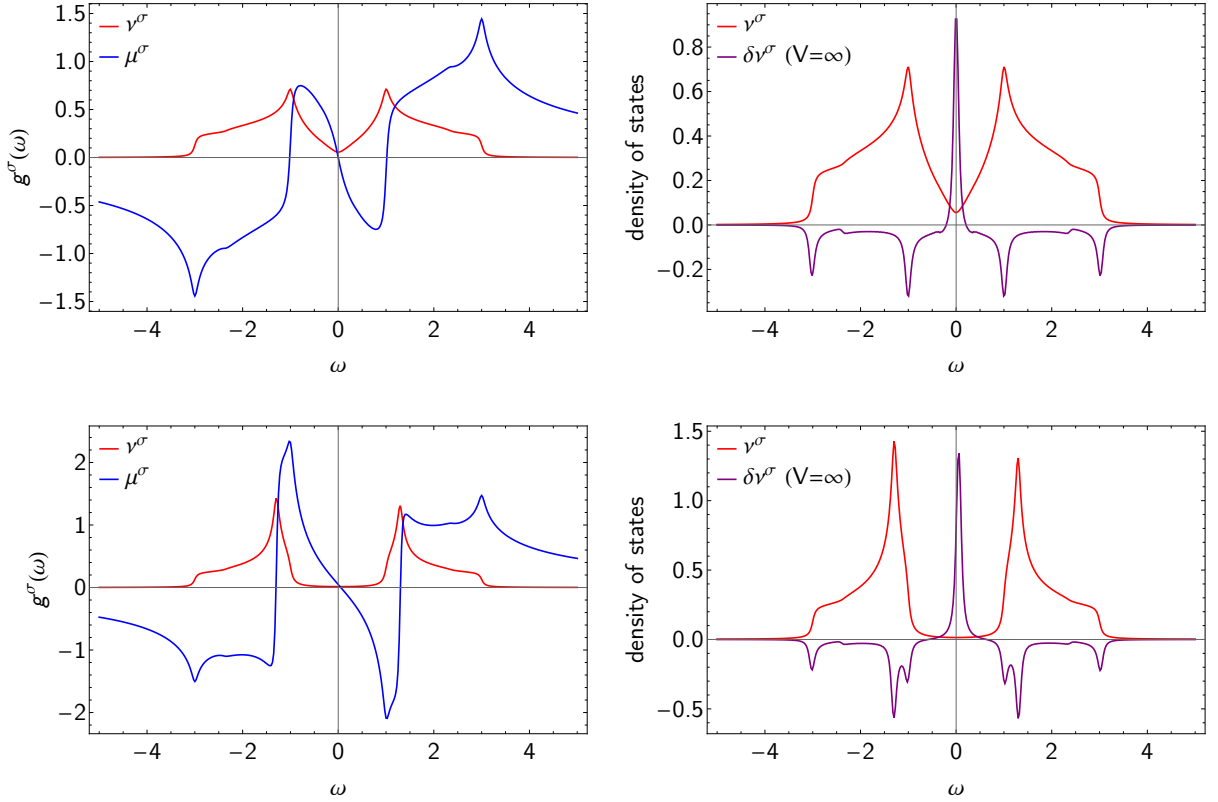


Figure 15. Local projected Green's function for the Kane-Mele model, coinciding with graphene for  $\beta = 0$  (top row) and with a  $\mathbb{Z}_2$  topological insulator with  $\beta = 1$  (bottom row). The ingap ring state in the gapped phase of the Kane-Mele model has the same origin as the Dirac point resonant state known to exist for vacancies in graphene.

We can consider a vacancy in a single site  $\mathbf{q}_0$  located in one of the sublattices, which affects a Kramer's pair,

$$\mathcal{V} = v \left( \left| \phi_0^\uparrow \right\rangle \left\langle \phi_0^\uparrow \right| + \left| \phi_0^\downarrow \right\rangle \left\langle \phi_0^\downarrow \right| \right) \quad (\text{E9})$$

which will lead to the appearance of a Kramers pair of ring states at  $E = 0$  in the strongly coupled impurity limit. An

index theorem [56] guarantees the symmetric spectrum, and the zero energy state can be understood by the fact that a state of definite sublattice is equally spread over the filled and empty bands. Therefore the level repulsion from the band into the ring state of definite sublattice is identical from both bands. In Fig.15 we plot the impurity projected local Green's function for two values of  $\beta$ , which determine the gap. Interestingly, we find that the zero energy state is robust independently of the magnitude of the spectral gap. In the Dirac semimetal limit, the ring state becomes the well-known zero-energy resonance expected in graphene [31].

We can appreciate from the present analysis that the topological protection of the ring states originates from the Wannier obstruction of the filled bands to construct symmetric states at a given sublattice and that the spectral fixed point generated by a local impurity cannot be removed by closing the spectral gap, but rather it is protected by the entire bandwidth of the bands. In the next appendices, we discuss how the zeros in  $\mu^\sigma(\omega)$  emerge in topologically obstructed bands.

### Appendix F: Wannier obstruction and orbital projected states

Let us consider the flattened Bloch Hamiltonian defined by the band projector as

$$\mathcal{H} = \sum_{\alpha} \varepsilon_{\alpha} \mathbb{P}^{\alpha}, \quad \mathbb{P}^{\alpha} = \sum_{\mathbf{k}} |\psi_{\alpha\mathbf{k}}\rangle \langle \psi_{\alpha\mathbf{k}}|. \quad (\text{F1})$$

A topological obstruction implies that it cannot be adiabatically connected to any flat band atomic limit, whose flat band Hamiltonian is defined by

$$\mathcal{H}_{\text{AL}} = \sum_{\sigma} \varepsilon_{\sigma} \mathbb{P}^{\sigma}, \quad \mathbb{P}^{\sigma} = \sum_i |\phi_i^{\sigma}\rangle \langle \phi_i^{\sigma}| \quad (\text{F2})$$

for  $\sigma$  a local orbital that preserves the local site symmetry group of the site  $\mathbf{q}_i$  [6]. Both Hamiltonians preserve the same spatial and internal symmetries. The possible  $\mathcal{H}_{\text{AL}}$  are exhaustively classified [1], and each band  $\mathbb{P}^{\sigma}$  transforms under a band representation of the space group [41, 42].

Focusing on a specific band  $\mathbb{P}^{\alpha}$  and a specific atomic limit  $\mathbb{P}^{\sigma}$  of the same dimension, if there is an adiabatic deformation between the two implies then there is a smooth and periodic unitary transformation  $U$  such that

$$\mathbb{P}^{\alpha} = U \mathbb{P}^{\sigma} U^{\dagger} \quad (\text{F3})$$

whose (diagonal) matrix elements in the momentum representation  $U(\mathbf{k}) = \langle \mathbf{k} | U | \mathbf{k} \rangle$  are smooth and periodic. A simple diagnosis of whether such unitary transformation exists was proposed in [43] by considering the projected states

$$|\Upsilon_i^{\sigma\alpha}\rangle \equiv \mathbb{P}^{\alpha} |\phi_i^{\sigma}\rangle = \mathbb{P}^{\alpha} \mathbb{P}^{\sigma} |\mathbf{q}_i\rangle \quad (\text{F4})$$

where  $|\mathbf{q}_i\rangle$  is a position eigenstate. Ref. [43] proposes to check their linear (in)dependence. Namely, if  $U$  does not exist, the projected states  $|\Upsilon_i^{\sigma\alpha}\rangle$  necessarily span a space *smaller* than the original band, which means that the overlap matrix

$$S_{ij} = \langle \Upsilon_i^{\sigma\alpha} | \Upsilon_j^{\sigma\alpha} \rangle \quad (\text{F5})$$

is singular with  $\det S = 0$ , with irremovable zero eigenstates. The diagonal entries of  $S_{ij}$  correspond to the norm of the projected states,  $s_{\alpha} = \langle \Upsilon_i^{\sigma\alpha} | \Upsilon_i^{\sigma\alpha} \rangle$ . Since  $\mathbf{q}_i$  form a lattice of symmetry-related sites,  $\mathbf{q}_i = g_{ij} \mathbf{q}_j$  for  $g_{ij}$  an element of the space group, it follows that the norm  $s_i$  is independent of the lattice site. Inserting (F4) into (F5) we can write the overlap matrix in the following form

$$S_{ij} = \langle \mathbf{q}_i | \mathbb{S} | \mathbf{q}_j \rangle \quad (\text{F6})$$

where  $\mathbb{S}$  is the positive semidefinite overlap operator, which we define in a basis independent way as follows

$$\mathbb{S} \equiv (\mathbb{P}^{\alpha} \mathbb{P}^{\sigma})^T (\mathbb{P}^{\alpha} \mathbb{P}^{\sigma}). \quad (\text{F7})$$

Its singular nature implies that

$$\text{rk } \mathbb{S} < \text{rk } \mathbb{P}^{\alpha} = \text{rk } \mathbb{P}^{\sigma} \quad (\text{F8})$$

Since both  $\mathbb{P}^\alpha$  and  $\mathbb{P}^\sigma$  are diagonalized in the momentum basis,

$$s_{\alpha\mathbf{k}}^\sigma = \langle \mathbf{k} | \mathbb{S} | \mathbf{k} \rangle = \sum_{ij} \exp\{i\mathbf{k} \cdot (\mathbf{q}_i - \mathbf{q}_j)\} S_{ij} = |\langle \sigma | \psi_{\alpha\mathbf{k}} \rangle|^2 \quad (\text{F9})$$

which necessarily vanishes for some value of  $\mathbf{k}$ . While it is possible that  $s_{\alpha\mathbf{k}}^\sigma$  has zeros that are not topologically protected, the topological statement is that at least one of these zeros is irremovable, for any choice of symmetric, periodic and smooth unitary rotation  $U$  we may do either in  $\mathbb{P}^\sigma$  or  $\mathbb{P}^\alpha$ .

The lack of an exponential localized Wannier basis of a given orbital character can be seen by trying to construct it explicitly from the projected states. These are not orthogonal. The orthogonalization process [57] gives a set of orthogonal states

$$|w_i\rangle = \sum_{ij} [S^{-1/2}]_{ij} |\Upsilon_j\rangle \quad (\text{F10})$$

which can only be constructed as long as  $\det S \neq 0$ . Rotating the atomic band by any smooth  $U$  will not solve this problem. Therefore, the Wannier functions defined by

$$|w_i\rangle = \sum_{\mathbf{k}} e^{i\mathbf{k} \cdot \mathbf{q}_i} e^{i\chi(\mathbf{k})} |\psi_{\alpha\mathbf{k}}\rangle \quad (\text{F11})$$

for an arbitrary smooth and periodic phase  $\chi(\mathbf{k})$  cannot be described as exponentially localized orbitals and necessarily decay algebraically away from their center at  $\mathbf{q}_i$  [6]. The lack of exponential localization of any choice of symmetric  $|w_i\rangle$  is reflected in the impossibility of orthogonalizing the projected states  $|\Upsilon_i^{\sigma\alpha}\rangle = \mathbb{P}^\alpha \mathbb{P}^\sigma |\mathbf{q}_i\rangle$  for any symmetry allowed choice of  $\mathbb{P}^\sigma$ .

A second necessary ingredient for our discussion is that

$$\sum_{\alpha} \mathbb{P}^\alpha = \sum_{\sigma} \mathbb{P}^\sigma = \mathbb{1} \quad (\text{F12})$$

which implies in particular that for every point in the Brillouin zone,

$$\sum_{\alpha\mathbf{k}} s_{\alpha\mathbf{k}}^\sigma = 1 \quad (\text{F13})$$

which can be read in the following way: if the projected weight of the band generated by the basis state  $|\phi_0^\sigma\rangle$  vanishes at some momentum in one Bloch band, it must be nonzero in another band across a topological gap. Note that in our notation

$$s_\alpha = \frac{1}{N} \sum_{\mathbf{k}} s_{\alpha\mathbf{k}}^\sigma \quad (\text{F14})$$

such that the small case  $s$  are always valued between 0 and 1.

## Appendix G: Topological stability of ingap ring states

In this section, we prove that a Wannier obstruction leads to the existence of finite energy zeros of the real part of the impurity projected Green's function  $\mu^\sigma(\omega)$ , corresponding to spectral attractors in the presence of strongly coupled perturbations. Our proof comes in two steps. First, we consider the flat band limit and show that a zero of  $\mu^\sigma(\omega)$  must exist in the topological gap. Second, we show that ingap zeros cannot be removed adiabatically.

### 1. Necessity of zeros in $\mu(\omega)$ in a topological gap

Let us consider a topological flat band Hamiltonian defined by the projector

$$\mathcal{H} = \sum_{\alpha} \varepsilon_{\alpha} \mathbb{P}^{\alpha}, \quad \mathbb{P}^{\alpha} = \sum_{\mathbf{k}} |\psi_{\alpha\mathbf{k}}\rangle \langle \psi_{\alpha\mathbf{k}}|. \quad (\text{G1})$$

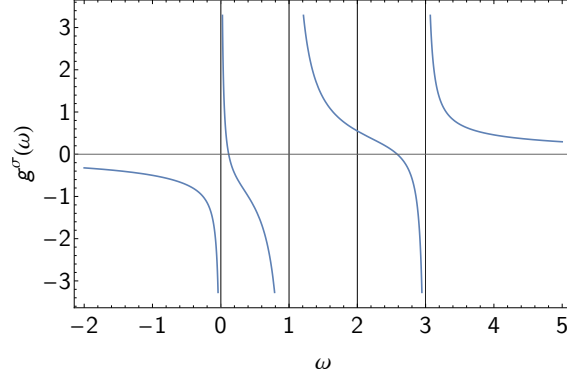


Figure 16. Example of the impurity projected Green's function for a four-band flat band Hamiltonian characterized by  $s_\alpha = (0.1, 0.7, 0, 0.2)$  at energies  $\varepsilon_\alpha = (0, 1, 2, 3)$ . Only the bands at energies 0, 1 and 3 are visible to the impurity  $\mathcal{V}$ .

The resolvent Green's function is given by

$$\mathcal{G}(\omega) = \sum_{\alpha} \frac{\mathbb{P}^{\alpha}}{\omega - \varepsilon_{\alpha}} \quad (\text{G2})$$

where all the poles collapse into a single energy  $\varepsilon_{\alpha}$ . For a rank 1 impurity of the form  $\mathcal{V} = v |\phi_0^{\sigma}\rangle \langle \phi_0^{\sigma}|$ , the impurity projected Green's function is given by

$$g^{\sigma}(\omega) = \sum_{\alpha} \frac{s_{\alpha}}{\omega - \varepsilon_{\alpha}} \quad (\text{G3})$$

giving a residue of  $s_{\alpha} = N^{-1} \text{tr} \mathbb{P}^{\alpha} \mathbb{P}^{\sigma}$  with  $N$  the number of states in the band. The pole weights satisfy  $0 \leq s_{\alpha} \leq 1$  and  $\sum_{\alpha} s_{\alpha} = 1$ , which assumes, without loss of generality, that there is a single  $\sigma$  orbital per site in the system.

If there is a topological obstruction, then  $s_{\alpha} < 1$  for all  $\alpha$  and  $s_{\alpha} > 0$  for at least two bands separated by a topological gap. Keeping only bands for which  $s_{\alpha} \neq 0$ , we get,

$$g^{\sigma}(\omega) = \sum_{\alpha: s_{\alpha} \neq 0} \frac{s_{\alpha}}{\omega - \varepsilon_{\alpha}} \quad (\text{G4})$$

we can see immediately that  $g^{\sigma}(\omega)$  has an opposite sign below and above the band, corresponding to a  $\pi$  shift across  $\varepsilon_{\alpha}$ . In between essential bands, there are topologically robust zeros of  $\mu^{\sigma}(\omega) = \text{re} g^{\sigma}(\omega - i0^+)$  at energies  $E_a$  confined to the gap between the bands. These zeros satisfy  $\partial_{\omega} \mu^{\sigma}(\omega)|_{E_a} < 0$  which characterizes a spectral *attractor* in the sense discussed above. As  $v \rightarrow \pm\infty$  the spectrum of the perturbed Hamiltonian  $\mathcal{H} + \mathcal{V}$  will get a state pinned at these attractors in the form of a ring state.

## 2. Stability of zeros in $\mu^{\sigma}(\omega)$ in dispersive bands

We now claim that the attractive fixed point in the gap cannot be absorbed by a single band while preserving the symmetry, and it can only be removed by closing a gap between bands. Here we argue this is the case in a few different ways. First, let us assume the zero exists at an ingap energy  $E_a$ , crossing zero with a negative slope  $\mu^{\sigma'}(E_a) < 0$  where the prime indicates derivative with respect to the energy, reaching the conduction band edge, which we set without loss of generality to be  $\varepsilon^{\text{min}} = 0$ , with a negative value  $\mu^{\sigma}(0) < 0$ . Since we know that above the conduction band  $\mu^{\sigma}(+\infty) > 0$ , we know there is a zero of positive slope at an energy  $E_r > 0$  inside the conduction band,  $\mu^{\sigma'}(E_r) > 0$ . Here the subscripts indicate “attractor” or “repeller” according to the sign of the slope of  $\mu^{\sigma}(\omega)$ . We may ask, can the zero of the band and the zero of the gap come together and annihilate each other, effectively removing the ingap spectral attractor without a topological, or band gap closing, phase transition? The answer is *no*. To see this, we note that if such a point would exist, the two zeros, the attractor, and the repeller would meet at the band edge (or slightly above) with zero slope, satisfying at the annihilation point

$$\mu^{\sigma}(E_a) = \mu^{\sigma}(E_r) = 0, \quad \mu^{\sigma'}(E_a) = \mu^{\sigma'}(E_r) = 0 \quad (\text{G5})$$

To see if this is possible, let us assume the density of states at the conduction band. Namely, we say that  $\nu^\sigma(\omega) \sim \omega^\gamma$  with  $\gamma \geq 0$ , for  $\omega$  defined from 0 up to a maximum value of  $W$ , the conduction bandwidth, such that the total number of states that match the impurity character is  $n = W^{1+\gamma}/(1+\gamma)$ .

We can write  $\mu^\sigma(\omega)$  as a function of the density of states of the valence and conduction bands separately,

$$\mu^\sigma(\omega) = \frac{1}{\pi} P \int d\omega' \frac{\nu^\sigma(\omega')}{\omega - \omega'} = \mu_v^\sigma(\omega) + \frac{1}{\pi} P \int_0^W d\omega' \frac{\nu^\sigma(\omega')}{\omega - \omega'} \quad (\text{G6})$$

where the first term is finite,  $\mu_v^\sigma(\omega) \sim 1/(\omega - \varepsilon_v)$  for  $\varepsilon_v \ll 0$  a representative energy of the valence band, and therefore at  $\omega$  close to the conduction band  $\omega \sim 0$  is just a finite positive number. Similarly,  $\mu_v^{\sigma'}(\omega) \sim -1/(\omega - \varepsilon_v)^2$ , which is a finite negative number at the band edge. The second term may be divergent at the band edge, and therefore we focus on it. Looking at the slope of  $\mu(\omega)$  as we approach the band edge from below  $\omega \rightarrow 0^-$ , we find that

$$\mu^{\sigma'}(\omega) = \mu_v^{\sigma'}(\omega) + \int_0^W d\omega' \frac{\nu^{\sigma'}(\omega')}{\omega - \omega'}. \quad (\text{G7})$$

For  $\gamma = 0$ , the density of states is constant, and its derivative at small  $\omega$  given by  $\nu'(\omega) = \delta(\omega)$ . This corresponds to a usual band edge with an effective mass in two dimensions. In this case, the slope of  $\mu(\omega)$  diverges as  $\mu'(\omega) \sim 1/\omega$ , and approaching it from below, the slope will always be negative, and therefore it is not possible to satisfy (G5).

Since we look at the impurity projected density of states, a step function is not necessarily the correct choice. Let us say that it grows linearly,  $\nu(\omega) \sim \omega$ . In this case,  $\mu'(\omega) \sim \log(1 - W/\omega)$ , with a logarithmic divergence at the band edge, and therefore  $\mu'(0^-) < 0$  and the condition (G5) cannot be satisfied. For larger powers  $\gamma > 1$ , the density of states grows very slowly, and we can expect that the condition (G5) may be satisfied. However, the limit is well defined and can be computed in a closed form

$$\lim_{\omega \rightarrow 0^-} \mu^{\sigma'}(\omega) \sim -\frac{\gamma}{\gamma - 1} W^\gamma. \quad (\text{G8})$$

That is, at a band edge,  $\mu^{\sigma'}(\omega)$  is *strictly negative* for any algebraic growth of the density of states  $\nu^\sigma \sim \omega^\gamma$ . Therefore, it is impossible to satisfy (G5) at a band edge. The only way to remove the additional zeros created at the topological phase transition is to close the gap between the conduction and valence bands. We can see the topological phase transition in Figs.14 and 13. At that point two concurrent things happen: the repeller annihilates the attractor, and the band gap closes. Importantly we note that the repeller of the lower band remains unaffected across the transition.

In conclusion, the number of finite energy spectral attractors is stable against dispersion deformations, and cannot be changed adiabatically, unless  $\nu^\sigma$  is made to fully vanish within the band. This is only possible if a topological obstruction does not prevent it.

### 3. Topologically enforced adiabatic discontinuity between unperturbed and perturbed bands

We now show that the ring state, even if it enters the band continuum, turns into a resonance which cannot be adiabatically removed. That is, the finite energy attractor in  $\mu^\sigma(\omega)$  necessarily remains even if the bulk density of state is finite  $\nu^\sigma(\omega)$  at its energy.

Let us first consider the case the attractor does not overlap with the band, such that the perturbed band is composed of extended scattering eigenstates  $|\tilde{\psi}_n^\alpha\rangle$ , which assume the general form [52]

$$|\tilde{\psi}_\mathbf{k}^\alpha\rangle = |\psi_\mathbf{k}^\alpha\rangle + \mathcal{G}(E - i0^+) \mathcal{V} |\tilde{\psi}_\mathbf{k}^\alpha\rangle, \quad (\text{G9})$$

with  $|\psi_\mathbf{k}^\alpha\rangle$  the unperturbed Bloch states. Independently of spatial dimension, in a finite size lattice with  $N$  sites if a rank-1 impurity  $\mathcal{V}$  is strongly coupled to the band, that is  $\mathcal{G}(E - i0^+) \mathcal{V}$  has an eigenstate of order  $O(1)$  when  $v \rightarrow \infty$ , it leads to a  $\pi$  shift across the band from the removal of a single states from the band continuum. There are only  $N - 1$  solutions of the type in (G9), stemming from the zeros of  $\mathcal{G}(\omega)$  in between the unperturbed poles. On the other hand, if the perturbation caused by  $\mathcal{V}$  on the band is weak, there is no bound state removed from the band and the sign of  $g(\omega)$  is the same on both edges of the band, a zero overall phase shift. In this case Eq.G9 has  $N$  solutions corresponding to weakly perturbations from the original Bloch states. For  $v \rightarrow \pm\infty$ , let us write formally the band projector operator at  $v \rightarrow \infty$ ,

$$\tilde{\mathbb{P}}^\alpha = \sum_{n=1}^{N-1} \left| \tilde{\psi}_\mathbf{k}^\alpha \right\rangle \left\langle \tilde{\psi}_\mathbf{k}^\alpha \right| \quad (\text{G10})$$

The projector into the perturbed topological band is related to the unperturbed ones by

$$\sum_{\alpha} \tilde{\mathbb{P}}^{\alpha} + |\sigma_E\rangle \langle \sigma_E| + |\rho_E\rangle \langle \rho_E| = \sum_{\alpha} \mathbb{P}^{\alpha} = \mathbb{1}. \quad (\text{G11})$$

Bracketing both sides of the completeness equality (G11) with the impurity eigenstate  $|\sigma\rangle$ , we find in the limit  $v \rightarrow \pm\infty$

$$\sum_{\alpha} \langle \sigma | \tilde{\mathbb{P}}^{\alpha} | \sigma \rangle + 1 = \sum_{\alpha} s_{\alpha} = 1 \quad (\text{G12})$$

where we used  $|\langle \sigma | \sigma_E \rangle|^2 \rightarrow 1$  and  $|\langle \sigma | \rho_E \rangle|^2 \rightarrow 0$ . Eq.G12 implies that  $\langle \sigma | \tilde{\mathbb{P}}^{\alpha} | \sigma \rangle = 0$  for every band  $\alpha$  of the perturbed system. This is simply a restatement that  $|\sigma_{E=\infty}\rangle = |\sigma\rangle$  is an eigenstate of the perturbed Hamiltonian  $\tilde{\mathcal{H}}$  with an energy far beyond the band energies.

Let us choose without loss of generality to bring the ring state  $|\rho_E\rangle$  into the (empty) band  $\alpha = 2$ . If it is possible to remove the zeros of  $\mu^{\sigma}(\omega)$  by annihilating one attractor and one repeller at the empty band, the perturbation  $\mathcal{V}$  did not remove a state from the band, and all the perturbed states in the band can be adiabatically deformed back into clean Bloch states. That is,  $\tilde{\mathbb{P}}^{\alpha=2} + |\rho_E\rangle \langle \rho_E|$  must span the same space as  $\mathbb{P}^{\alpha=2}$ . On the other hand, from completeness, also the perturbed filled band  $\tilde{\mathbb{P}}^{\alpha=1}$  together with the state  $|\sigma_E\rangle$  must span the same space as the unperturbed filled band  $\mathbb{P}^{\alpha=1}$ . That is, we have shown that in the limit  $v \rightarrow \infty$ , if the ring state can be absorbed by one of the topological bands, the local state  $|\sigma_{E=\infty}\rangle = |\sigma\rangle$  must be contained in the unperturbed band subspace  $\mathbb{P}^{\alpha=1}$  of the other topological band, which is a contradiction.

We have proven in the previous paragraph that the attractor of  $\mu^{\sigma}(\omega)$  cannot be removed simply by absorbing it into one band. The ring state is robust to any spectral deformation that will not re-invert the bands by removing the additional zeroes of  $\mu^{\sigma}(\omega)$  created at the phase transition. Note that if the attractor is buried into a band, it will result in a resonance, which means that when the ring state overlaps with the band it gains a finite lifetime [52] given by

$$\Gamma(E) = \frac{\nu^{\sigma}(E)}{\mu^{\sigma'}(E)}. \quad (\text{G13})$$

Let us consider for example graphene [31], which we have seen in Fig.15 to retain its attractor at the Dirac point even if the gap is fully closed. The ring state in this case gains a polynomial decay and has with infinite lifetime only at  $v = \pm\infty$  since at the Dirac point  $\nu^{\sigma}(\omega)$  vanishes. For any smaller  $v$  the resonance is slightly shifted above or below the Dirac point and gains a finite lifetime. Alternatively, when the density of states grows slower than a linear,  $\gamma > 1$ , it is possible that the attractor moves into the band. This is expected for three dimensional Weyl semimetals where  $\nu(\omega) \propto \omega^2$  at energies close to the Weyl point. The resonance expected in this case is also topologically protected.

## Appendix H: Exact solutions for ring state wavefunctions in the two-dimensional Chern insulator

Let us now look at the spatial profile of the ring state in the gap between Chern bands by finding the analytical expression to the local Green's function in the continuum model (E4)

$$h(\mathbf{k}) = (m + bk^2)\sigma_z + v\mathbf{k} \cdot \boldsymbol{\sigma} \quad (\text{H1})$$

close to a topological phase transition for small  $m$ . This exercise will let us understand which elements contribute to the short and long-distance behavior of the ring state wavefunction. In real space, the bare Green function may be written as

$$\mathcal{G}(\omega; \mathbf{r}, 0) = \langle \mathbf{r} | \mathcal{G}(\omega) | 0 \rangle = \int \frac{d\mathbf{k}}{(2\pi)^2} \frac{\omega\sigma_0 + (m + bk^2)\sigma_z + v\mathbf{k} \cdot \boldsymbol{\sigma}}{\omega^2 - (m + bk^2)^2 - v^2k^2} e^{i\mathbf{k} \cdot \mathbf{r}} \quad (\text{H2})$$

Let us rewrite the denominator as  $-b^2(k^2 + k_1^2)(k^2 + k_2^2)$  where  $k_1^2, k_2^2$  are defined by the zeroes of the denominator,  $k_1 = \sqrt{m^2 + \omega^2}/v$  and  $k_2 = v/b$ . We observe that  $k_1$  and  $k_2$  define two natural length scales in the Hamiltonian (E4). First, at small momenta and large distances,  $k < k_2$ , the orbital character of the filled band is determined by the sign of the mass  $m$ . Second, at large momenta or small distances,  $k > k_1 = v/b$ , the sign of  $b$  determines the orbital character. When  $b$  and  $m$  have opposite signs, there is a band inversion leading to a topologically nontrivial band characterized by a Chern number. The two momenta define a band inversion scale  $k_{\text{inv}} = \sqrt{k_1 k_2} = \sqrt{m/b}$ , for which the orbital character is fully mixed.

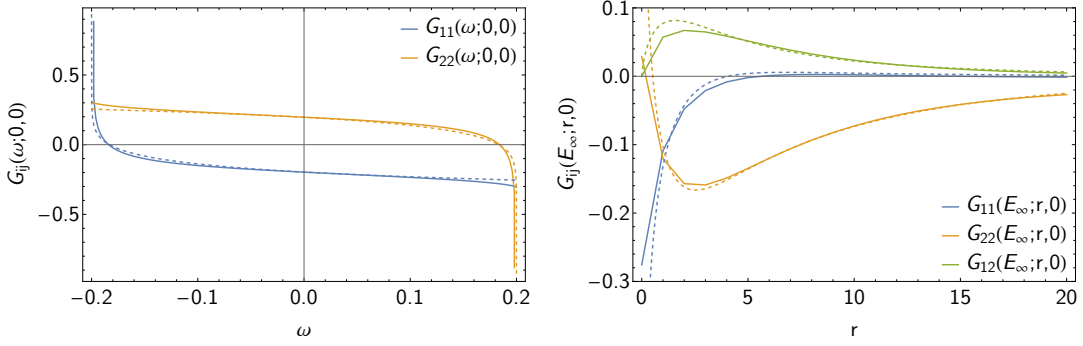


Figure 17. Comparison between the numerical calculation of  $\mathcal{G}_{ij}(\omega; r, 0)$  from the tight-binding model in a mesh of  $200 \times 200$  sites in the Brillouin zone, and analytical expressions of the ingap Green's function in the continuum approximation. We use a cutoff value of  $\Lambda = 5$  at  $r = 0$  and no cutoff in the right figure, which means we can see the nonphysical logarithmic divergence as  $r \rightarrow 0$ . Both figures are in the Chern phase with  $m = -0.2$ ,  $b = 1.5$ , and  $v = 1$ . Here the zero energy is given by  $E_\infty = 0.184$ .

Let us first calculate  $\mathcal{G}(\omega; 0, 0)$ , which is pathological without a lattice regularization. To do so, we must truncate the integral at large momenta by a momentum cutoff  $\Lambda$ . We find

$$\mathcal{G}(\omega; 0, 0) = -\frac{1}{2\pi b^2} \int_0^\Lambda dk k \frac{\omega \sigma_0 + (m + bk^2) \sigma_z}{(k^2 + k_1^2)(k^2 + k_2^2)}. \quad (\text{H3})$$

This integral can be divided into two contributions  $\mathcal{G}(\omega; 0, 0) = -(A_0 + bB_0)/(2\pi b^2)$  with

$$A_0 = \frac{\omega \sigma_0 + m \sigma_z}{k_1^2 - k_2^2} \log(k_1/k_2) \quad (\text{H4})$$

and

$$B_0 = \left( \frac{k_1^2 \log k_1 - k_2^2 \log k_2}{k_1^2 - k_2^2} + \log \Lambda \right) \sigma_z \quad (\text{H5})$$

The logarithmic divergence of  $\mathcal{G}(\omega; 0, 0)$  is not present for the lattice problem, and we can fix the cutoff to fit the numerical result.

The analytical expressions can be compared to the numerical calculation of Green's function in Fig.17

Let us now look at the radial dependence of the Green's function by decomposing the operator  $\mathcal{G}(\omega; \mathbf{r}, 0)$  into a diagonal and an off-diagonal part. The diagonal terms of the integral depend only on the radial component of  $\mathbf{r}$ , which becomes

$$\mathcal{G}(\omega; r, 0)_{\text{diag}} = -\frac{1}{2\pi b^2} \int_0^\Lambda dk k J_0(kr) \frac{\omega + (m + bk^2) \sigma_z}{(k^2 + k_1^2)(k^2 + k_2^2)} \quad (\text{H6})$$

where  $J_0(x)$  is the Bessel function of the first kind. The first two terms in the sum can be easily integrated by utilizing the relation

$$\frac{1}{(k^2 + k_1^2)(k^2 + k_2^2)} = \frac{1}{(k_2^2 - k_1^2)} \left[ \frac{1}{k^2 + k_1^2} - \frac{1}{k^2 + k_2^2} \right] \quad (\text{H7})$$

Then, the integral is tabulated, and it can be explicitly written as  $\mathcal{G}(\omega; 0, 0) = -(A + bB)/(2\pi b^2)$  with

$$A = -\frac{\omega \sigma_0 + m \sigma_z}{k_1^2 - k_2^2} [K_0(k_1 r) - K_0(k_2 r)] \quad (\text{H8})$$

Note that as the energy reaches the gap  $\omega \rightarrow \pm m$ ,  $A$  vanishes for one of the diagonal entries. The third term in the integral may be calculated by noticing that the  $bk^2$  in the numerator is nothing but  $-b\nabla^2 = -b(\partial_r^2 + \frac{1}{r}\partial_r)$ . Then, using,  $\nabla^2 K_0(kr) = k^2 K_0(kr)$  the third term becomes

$$B = \frac{k_1^2 K_0(k_1 r) - k_2^2 K_0(k_2 r)}{(k_1^2 - k_2^2)} \sigma_z. \quad (\text{H9})$$

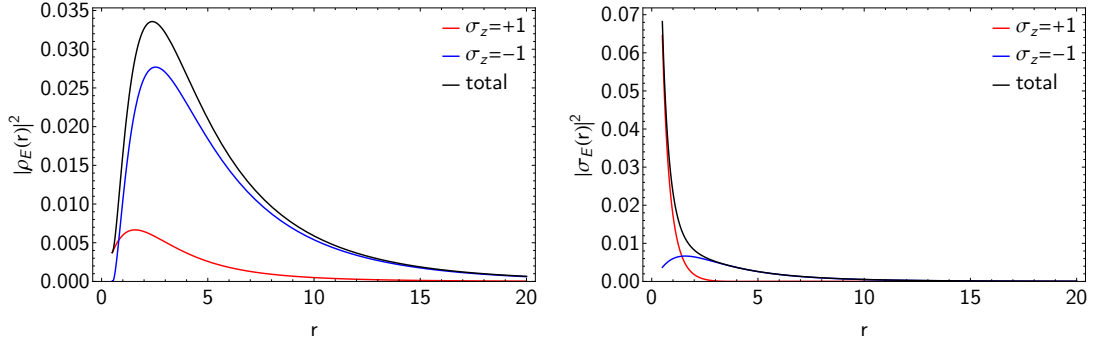


Figure 18. Radial profile and orbital content of two impurity eigenstates expected at the same ingap energy  $E = -0.184$ : (left) Ring state induced by an impurity with character  $\sigma_z = -1$  and infinite strength  $v$ ; (left) A band-edge impurity state induced by an impurity with character  $\sigma_z = +1$  and impurity strength  $v = 3.57$ . Parameters used are the same as in Fig. 17.

Finally, we have  $\mathcal{G}(\omega; r, 0)_{\text{diag}} = A + bB/(2\pi b^2)$ .

Note that the diagonal elements diverge logarithmically at  $r = 0$ . This is an ultraviolet divergence, which could be regularized in one of two ways: either cut it off by making the  $K_0(kr) \sim K_0(k/k_2)$  for  $r < 1/k_2$  (the short distance cut-off, or add a quartic ( $k^4$ ) term to the dispersion. This divergence is not present in the tight-binding model, and it is not important. After regularizing the ultra-violet divergence, the diagonal elements have three regimes: Around  $1/k_2$  they are constant (short scale). Between  $1/k_2$  to  $1/k_1$  (intermediate scale) they decrease logarithmically with  $r$ , and after that (long scale) they go down exponentially. The short scale is dominated by the  $k_2^2 K_0(k_2 r)$  term while the long scale term is dominated by the  $k_1^2 K_0(k_1 r)$  term, so these elements of the Green function change sign as  $r$  grows.

Finally, the off-diagonal terms of the Green's function  $\mathcal{G}(\omega; \mathbf{r}, 0)_{\text{off-diag}} = C/(2\pi b^2)$  can be written as

$$C = \int d\mathbf{k} \frac{v(\sigma_x \partial_x + \sigma_y \partial_y) e^{i\mathbf{k} \cdot \mathbf{r}}}{(k^2 + k_1^2)(k^2 + k_2^2)} = (e^{i\varphi} \sigma_+ + e^{-i\varphi} \sigma_-) \frac{vk_1 K_1(k_1 r) - vk_2 K_1(k_2 r)}{2(k_1^2 - k_2^2)} \quad (\text{H10})$$

where we use  $\mathbf{r} = r e^{i\varphi}$  and  $\sigma_{\pm} = \sigma_x \pm i\sigma_y$ . These terms do not diverge at  $r = 0$ ; rather, they start as  $r \log r$  at the short scale, continue as  $1/r$ , and then decay exponentially. At the long scale all elements of the Green's function decay exponentially.

Let us now compute the ring state solution at  $E_{\infty}$ . We can compare the two type of solutions that exist at this energy, a weak impurity  $|\sigma_E\rangle$  and the strong impurity state  $|\rho_E\rangle$  both taken at  $E = E_{\infty}$ . For this, we start with

$$\varphi_E(\mathbf{r}) = \mathcal{G}(E; \mathbf{r}, 0)\varphi(0). \quad (\text{H11})$$

Noting that at  $E = E_{\infty} = -0.184$  there is a zero in  $\mathcal{G}_{11}$  but no zero at  $\mathcal{G}_{22}$ . That is, there is a zero in the projection  $g^1(E)$  but no zero in  $g^2(E)$ . At this energy, a local impurity affecting the orbital  $\mathcal{V} = v|\sigma = -1\rangle \langle \sigma = -1|$  with  $v = \infty$  will induce a ring state  $|\rho_E\rangle$ ; Also at this energy, a local impurity affecting the orbital  $\mathcal{V} = v|\sigma = +1\rangle \langle \sigma = +1|$  with  $v \sim 3.57$  will localize a band-edge impurity state  $|\sigma_E\rangle$ . The two states can be found by choosing  $\varphi(0) = |\sigma_z = \pm 1\rangle$ , and will show drastically distinct radial profiles. The result can be seen in Fig.18.